Current Topics in Electrochemistry

Review

The effect of different electrochemical treatments on the conduction properties of an elecroactive polymer: The case of poly(*o*-aminophenol)

Ricardo Tucceri*

Instituto de Investigaciones Fisicoquímicas Teóricas y Aplicadas (INIFTA), CONICET, Facultad de Ciencias Exactas, Universidad Nacional de La Plata, Sucursal 4, Casilla de Correo 16, (1900) La Plata, Argentina.

ABSTRACT

The effect of storage time without use (STWU) in the supporting electrolyte solution on the conducting properties of poly(*o*-aminophenol) (POAP) film electrodes was studied. Cyclic voltammetry (CV), rotating disc electrode voltammetry (RDEV), electrochemical impedance spectroscopy (EIS) and surface resistance (SR) were employed. The storage of a POAP film without use for time periods longer than 32 h strongly reduces its electroactivity. Here, this effect is called deactivation. The attenuation of the voltammetric response of the polymer film with the increase of the storage time allows one to define a degree of deactivation (θ_d). A decrease of the electron transport rate (D_e) with the increase of the degree of deactivation of POAP films was obtained from RDEV measurements. The relative surface resistance change ($\Delta R/R$) of a gold film coated with POAP is also attenuated by the increase of the STWU. Impedance spectra of deactivated and nondeactivated POAP films in the presence of an electroactive solution and in the sole presence of the supporting electrolyte were analyzed on the basis of two different impedance models. As the deactivation of POAP films by the STWU studied in this work was compared with deactivations caused by other electrochemical and chemical treatments, such as prolonged potential cycling (PPC), high positive potential limits (HPPL) and soaking in a ferric ion solution (SFeIS), this paper can be considered as a review, where the most significant studies that have been reported about the stability of POAP are documented.

KEYWORDS: poly(*o*-aminophenol) film electrodes, deactivation, storage time without use, prolonged potential cycling, high positive potential limits, soaking in a ferric ion solution.

INTRODUCTION

The oxidation of *o*-aminophenol (*o*-AP) over different electrode materials (gold, platinum, carbon, indium-tin oxide, etc.) in aqueous medium was shown to form poly-*o*-aminophenol (POAP) [1-3]. *O*-AP can be polymerized electrochemically in acidic, neutral and alkaline solutions. While a conducting film is only formed in acidic media, POAP synthesized in neutral and alkaline media leads to a nonconducting film [4]. The properties of POAP synthesized in basic medium are favorable to applications in the field of bioelectrochemistry and electrocatalysis [5]. The charge-transport process at POAP films synthesized in acid medium was mainly studied from the basic research viewpoint employing different electrochemical techniques [1, 3, 6, 7]. POAP synthesized in acidic medium is also found to be a useful material to build electrochemical sensors and electrocatalysts. The development of nitric oxide [8] and ferric cation [9]

*Email id: rtucce@inifta.unlp.edu.ar

sensors based on POAP synthesized in acid medium has been reported. POAP was also employed for the electrocatalytic detection of dihydronicotinamide adenine dinucleotides (NAD(P)H) [10], and for the reduction of dissolved oxygen [11]. Considering the interest in POAP synthesized in acid medium in both basic and applied research, not much attention has been paid to the decay of the electroactivity of POAP caused by its extensive use. It is often indicated that POAP films have good electrochemical properties in terms of conductivity and ion-permeability and also that they present good durability and long-term stability under storage during several weeks. In this regard, it is assumed that the reversible redox response and conducting properties of POAP remain substantially unchanged before and after it has been used. The aim of the present work is to demonstrate that charge-transport and charge-transfer parameters of POAP change with its storage when not used for prolonged time periods. Four techniques were employed in this work: cyclic voltammetry (CV), rotating disc electrode voltammetry (RDEV), electrochemical impedance spectroscopy (EIE) and surface resistance (SR) [12]. CV was employed to assess a degree of deactivation. RDEV data were analyzed in terms of the electron hopping model by assuming that the polymer deactivation by storage leads to an increase in the electron hopping distance between redox sites [13]. Impedance diagrams of POAP films after they were stored for different time periods were interpreted by employing two theoretical models: the first was used to obtain transport parameters when POAP contacts an electroactive solution and the second one was employed to analyze the impedance behavior of POAP films in the sole presence of the supporting electrolyte solution. The objective of the interfacial resistance measurements was to demonstrate the existence of different distributions of redox sites at deactivated POAP film electrodes as compared with nondeactivated ones. Changes in the redox site configuration after POAP deactivation by storage monitored by SR were associated with changes in the charge-transfer and charge-transport parameters obtained by employing RDEV and EIE. Charge-transfer and charge-transport parameters obtained in this work for POAP films deactivated by STWU are compared with those obtained in other works for POAP films deactivated employing other procedures such as, prolonged electrode potential cycling (PPC) [14], high positive potentials limits (HPPL) [15] and soaking a ferric ion solution (SFeIS) [16, 17]. It is expected that the present review paper will shed light on the limits of stability and durability of POAP, particularly when it is proposed as a material for developing sensors and electrocatalysts.

MATERIALS AND METHODS

Cyclic voltammetry (CV), rotating disc electrode voltammetry (RDEV), ac impedance and surface resistance (SR) experiments

A gold rotating disc electrode (RDE) was used as the base electrode to deposit POAP films. This gold RDE consisted of a gold rod press fitted with epoxy resin into a Teflon sleeve so as to leave a 1 cm^2 disc area exposed. The electrode was carefully polished with emery paper of decreasing grit size followed by alumina suspensions of 1, 0.3 and 0.05 μm, until a mirror-like finish was obtained. Then, it was submitted to ultrasonic cleaning to remove residual abraded polishing materials. In order to obtain a more specular gold surface to deposit POAP films, a gold film about 50 nm in thickness was deposited by vacuum evaporation [12] (~ 10^{-7} Torr) on the gold disc. The thickness of the evaporated gold thin film was determined as described in [12]. Then, in all experiments carried out in this work, POAP films were deposited on a specular gold film surface. The use of a specular metal surface (low roughness) to synthesize the polymer film allows one to interpret impedance data by employing a homogeneous electrochemical impedance model [18]. POAP films were grown on these base electrodes following the procedure described elsewhere [1, 2]. That is, polymer films were obtained by immersing the base electrode in a 10^{-3} M *ortho* aminophenol + 0.4 M $NaClO_4$ + 0.1 M $HClO_4$ solution and cycling the potential between -0.25 and 0.8 V (*versus* saturated calomel electrode (SCE)) at a scan rate $\nu = 0.05$ V s^{-1}. In the same way as in a previous paper [6], POAP films were grown up to an approximate thickness of $\phi_p \sim 60$ nm by using a reduction charge ($Q_{Red,T} = 2.8$ mC cm^{-2}) *versus* the ellipsometric thickness working curve [19]. These POAP-coated gold film electrodes were then rinsed and transferred to the supporting electrolyte solution (0.4 M $NaClO_4$ + 0.1 M $HClO_4$) free of

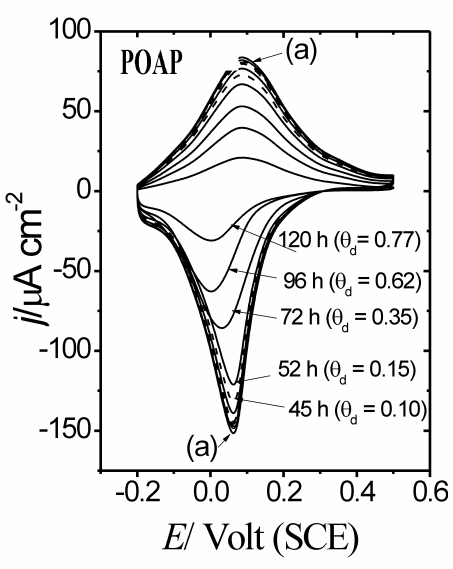

Fig. 1. Voltammetric (*j*-*E*) responses for a 2.8 mC cm^{-2} (ϕ_p = 60 nm) thick POAP film. (a) A nondeactivated POAP film (θ_d = 0). The other voltammetric responses correspond to POAP films which were held without use in the supporting electrolyte solution for the time periods indicated in the figure. The degrees of deactivation of the films are indicated in Table 1. Electrolyte: 0.1 M $HClO_4$ + 0.4 M $NaClO_4$. Scan rate: ν = 0.01 V.

monomer, where they were stabilized by a continuous potential cycling at a scan rate of 0.01 V s^{-1}. A typical voltammetric response of these films is shown in Fig. 1 (plot (a)). The POAP films maintain this response on potential cycling within the potential range -0.2 V < *E* < 0.5 V up to 500 cycles. These POAP films are herein called nondeactivated films. A large-area gold grid was used as counterelectrode. All the potentials reported in this work are referred to the SCE.

A series of eight POAP-coated RDE was prepared (see first column in Table 1) and each one of them was successively employed in an individual experiment. That is, each POAP film was stored without use in a deoxygenated supporting electrolyte solution for a given time period (see second column in Table 1) and then, it was cycled within the potential region –0.2 < *E* < 0.5 V to obtain a stable voltammetric response. Then, the corresponding *j*-*E* responses for each one of the eight POAP films were compared. An attenuation of the voltammetric response was observed for these films as the storage time increases beyond 32 h (Fig. 1). These POAP films are herein called

Table 1. Effect of the storage time without use in the supporting electrolyte solution on the voltammetric charge of a POAP film.

[a]POAP films	[b]Storage time/h	[c]$Q_{Red,c}$/mC cm^{-2}	[d]θ_c^d
1	32	2.65	0.05
2	45	2.52	0.10
3	52	2.37	0.15
4	60	2.10	0.25
5	72	1.83	0.35
6	83	1.67	0.41
7	96	1.12	0.62
8	120	0.62	0.77

[a]: Numbers 1 to 8 represent different deactivated POAP films.
[b]: Storage time (in hours) of each POAP film in the supporting electrolyte solution.
[c]: Voltammetric reduction charge of the different deactivated POAP films after being held without use in the supporting electrolyte solution for the time periods listed in column 2.
[d]: Degree of deactivation of each one of the POAP films after being held without use in the supporting electrolyte solution for the time periods listed in column 2. The degree of deactivation achieved by each film after storage was calculated from $\theta c^d = 1 - (Q_{Red,c}/Q_{Red,T})$, where $Q_{Red,T}$ (= 2.8 mC cm^{-2}) is the voltammetric reduction charge of a nondeactivated film.

deactivated films. Then, with both nondeactivated and deactivated by storage POAP films, RDEV and *ac* impedance experiments were performed in the presence of a solution containing equimolar concentrations of *p*-benzoquinone (Q) and hydroquinone (HQ) species (0.1 M $HClO_4$ + 0.4 M $NaClO_4$ + 2 x 10^{-3} M Q/HQ). Stationary current-potential curves (*I-E*) at different electrode rotation rates, Ω, were recorded. From these curves, cathodic and anodic limiting current *versus* electrode rotation rate (I_{lim} *versus* $\Omega^{1/2}$) dependences were obtained. Also, with nondeactivated and deactivated POAP films, *ac* impedance diagrams at the cathodic current plateaux were obtained for different electrode rotation rates. In some experiments the HQ/Q redox couple concentration in solution was varied. Impedance spectra of nondeactivated and deactivated POAP-coated electrodes in the sole presence of the supporting electrolyte solution (0.4 M $NaClO_4$ + 0.1 M $HClO_4$) were also recorded.

In CV and RDEV measurements a PAR Model 173 potentiostat and a PAR Model 175 (Princeton, USA) function generator were used. An X1-X2-Y Hewlett-Packard Model 7046 B plotter (Pasadena, California, USA) was used to record *j-E* and steady-state current-potential curves *I-E*. The electrode rotation speed, Ω, was controlled with a homemade equipment that allows one to select a constant Ω in the range 50 rev min^{-1} < Ω < 7000 rev min^{-1}. This was periodically controlled with a digital photo tachometer (Power Instruments Inc., model 891). Impedance spectra were measured following a 30-min application of the steady-state potential ranging from -0.35 V to 0.0 V.

Impedance values were determined at seven discrete frequencies per decade with a signal amplitude of 5 mV. The validation of the impedance spectra was done by using Kramers-Kronig transformations. Impedance measurements in the frequency range 0.01 Hz–10 kHz were performed with a PAR 309 system (Princeton, USA).

The experimental arrangement employed to perform surface resistance (SR) experiments is one in which a POAP film is supported on a rectangular thin gold film. Eight gold thin film electrodes of constant thickness ϕ_m ~ 30 nm were prepared by vacuum evaporation as described previously [12]. All these electrodes exhibit initial resistance (*R*) values of about 20.02 ohm. The relationship between the length *l* and the width *w* (*G* = *l*/*w*) of these gold film electrodes was 2. The electrode area was 1 cm^2. POAP films of 60 nm were grown on these base electrodes following the procedure previously described. A series of eight POAP-coated gold film electrodes was prepared and each one of them was successively employed in an individual experiment. That is, each POAP film was stored without use in a deoxygenated supporting electrolyte solution for the time periods indicated in Table 1. Then, the corresponding *j-E* and $\Delta R/R$-*E* responses for each one of the eight POAP films were recorded.

The experimental setup for simultaneous voltammetric and SR measurements on thin film electrodes has previously been described in detail [12]. The electrochemical cell also was the same as that described previously [20]. The electrode resistance change was measured employing the three contact method described earlier [20]. In this method, the voltage drop along the resistive electrode due to a constant current (I_m = 1 mA) applied to the extremes is measured. That is, in this method a current is fed through two contacts at the extremes of the rectangular thin film electrode while the third one, the central contact, is connected to the current follower of the potentiostat. The possibility of coupling between the faradaic and measuring currents into the electrode was taken into account in a previous paper [20]. It was demonstrated [20] that side effects of the faradaic current passing through the electrode can be neglected when the contacts at the ends of the electrode are symmetrically placed with respect to the central one. Then, the potential drop along the resistive electrode together with the polarization current is measured as a function of the applied potential *E*. The voltage difference at the extremes of the film is directly proportional to the resistance, and thus to the resistivity of the electrode. The potential drop along the extremes of the film was measured with a voltmeter. The output of the voltmeter was compensated employing a reference tension. In this was only resistance variations, ΔR (or ΔV potential variations), as a function of the electrode potential, *E*, are measured. ΔR changes around 10^{-4} ohm could be measured. Usually, the relative resistance change as a function of potential ($\Delta R/R$-*E*) is recorded in SR experiments, where *R* is a constant value. As indicated above, for a 30 nm thick gold film, the *R* value is 20.02 ohm.

A PAR Model 173 potentiostat together with a PAR Model 175 function generator were also used for potentiodynaic measurements. The potential drop at the extremes of the film was measured with a Keithley Model 160 voltmeter.

AR grade chemicals were used throughout. *O*-aminophenol (Fluka, Darmstadt, Germany) was purified as described elsewhere [1, 2]. $HClO_4$ and $NaClO_4$ (Merck, Darmstadt, Germany) were used without further purification. Benzoquinone and hydroquinone (Merck, Darmstadt, Germany) were also used without purification. The solutions were prepared with water purified using a Millipore Milli-Q system (Merck, Darmstadt, Germany).

RESULTS AND DISCUSSION

Voltammetric responses of nondeactivated and deactivated POAP films

The voltammetric response corresponding to a nondeactivated POAP film within the potential range comprised between -0.2 V and 0.5 V is shown in Fig. 1 (plot (a)). As indicated above, the POAP film maintains this response within the potential range -0.2 V < E < 0.5 V even after storage without use in the supporting electrolyte solution for 32 h. However, after a higher storage time this response starts to change. Fig. 1 compares the *j*-*E* responses of a nondeactivated POAP film (plots (a)) with those of the films (1), (2), (4), (5), (6) and (8) (see first column of Table 1) that were stored without use in the supporting electrolyte for the time periods listed in column 2 of Table 1. The more attenuated voltammetric response observed in Fig. 1, as the storage time increases indicates a deactivation of the POAP film. In this regard, the voltammetric reduction charge value corresponding to a nondeactivated film ($Q_{Red,T}$ = 2.8 mC cm^{-2}) was compared with each one of the reduction charges of the different deactivated films ($Q_{Red,c}$) indicated in Table 1. Then, a degree of deactivation (column 4 of Table 1) is defined as

$$\theta_c^d = 1 - (Q_{Red,c}/Q_{Red,T}) \quad (1)$$

In Eq. (1), $Q_{Red,c}$ is the total reduction charge assessed by integration of the corresponding *j*-*E* response from E = 0.5 V towards the negative potential direction for a deactivated film, and $Q_{Red,T}$ = 2.8 mC cm^{-2} is the total reduction charge for the nondeactivated film. In this way, for a nondeactivated POAP film (plot (a) in Fig. 1) the degree of deactivation was $\theta_c^d = 0$, taking $Q_{Red,T}$ = 2.8 mC cm^{-2} as reference charge. However, values of $\theta_c^d > 0$ are indicative of POAP films that have been deactivated by storage in the supporting electrolyte solution. Fig. 2 shows the dependence of the degree of deactivation of a POAP film on the storage time in the supporting electrolyte solution.

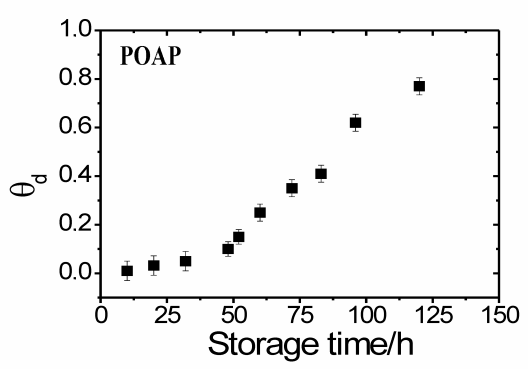

Fig. 2. Degrees of deactivation of a POAP film achieved after storage without use in the supporting electrolyte solution for the time periods indicted in Table 1.

Rotating disc electrode voltammetry and ac impedance measurements in the presence of an electroactive solution

As indicated above, RDEV and EIS were employed to study the behavior of nondeactivated and deactivated POAP films in contact with an electroactive solution containing the hydroquinone/ *p*-benzoquinone redox couple. In the presence of a redox active solution, besides charge transfer between redox sites of the polymer and the external redox couple, the oxidation and reduction of fixed sites introduce charged sites into the polymer film, which, in order to achieve charge neutrality, require the ingress of counterions from the contacting electrolyte solution and, according to the Donnan relation, the egress of co-ions. Disregarding the charge-transport control, a redox polymer undergoing electrolysis may follow Fick's diffusion law and usually Fick's formalism agrees with the experimental results. Electron hopping is believed to be the mechanism for electron transport in polymer materials, but it is also possible that ion motions may partially or totally control the rate of charge transport.

Then, steady-state current-potential curves were interpreted on the basis of the traditional electron hopping model [21, 22] and impedance spectra were analyzed employing the general theory of *ac* impedance described in a previous work [18], which allows one to obtain electron and ion diffusion coefficients and different interfacial (metal/polymer and polymer/solution) resistances and capacitances of an electroactive material.

In a previous work [23] RDEV experiments over gold electrodes coated with POAP films were carried out to study the diffusion processes of benzoquinone (*Q*) and hydroquinone (*HQ*) species through nondeactivated films. Diffusion-limited currents at $E < 0.0$ V for *Q* reduction and at $E > 0.8$ V for *HQ* oxidation were observed. While the anodic limiting current corresponds to the oxidation of *HQ* species that penetrate through the polymer film to reach the metal surface, cathodic limiting currents for *Q* reduction are related to a rapid electron-transfer mediation at the POAP|redox active solution interface, which occurs without significant penetration of *Q* into the polymer layer. As we use the theory of Vorotyntsev *et al*. [18] to interpret the impedance behavior of POAP films and as this theory was developed within the framework of the assumption that the redox active species are only present in the solution phase but not inside the film, and they participate in the interfacial electron exchange with the polymer at the film-solution boundary, only the electrochemical behavior of nondeactivated and deactivated POAP films at negative potential values ($E < 0.0$ V) was considered. Fig. 3 shows stationary current-potential curves (*I-E*) at different electrode rotation rates, Ω, for a nondeactivated POAP film in contact with a 0.1 M $HClO_4$ + 0.4 M $NaClO_4$ + 2 x 10^{-3} M Q/HQ solution. *I-E* curves at different Ω values were also obtained for each one of the deactivated POAP films indicated in Table 1. For instance, Fig. 4 shows this representation for a deactivated POAP film with $\theta_d = 0.62$. As can be seen by comparing Figs. 3 and 4, at each electrode rotation rate, both anodic and cathodic limiting currents for a deactivated POAP film are lower than those for a nondeactivated one. Also, after a given electrode rotation rate, which depends on the degree of deactivation, the cathodic limiting current for a deactivated film becomes independent of this

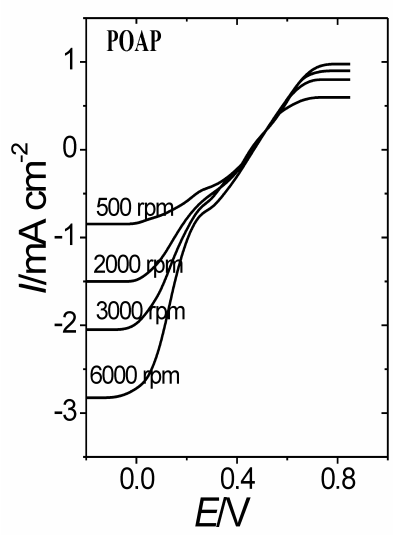

Fig. 3. Steady-state current-potential (*I-E*) curves for different rotation rates (Ω) of the rotating disc electrode. A nondeactivated POAP film. Ω values are indicated in the figure. Film thickness: 60 nm. Electrolyte: 0.1 M $HClO_4$ + 0.4 M $NaClO_4$+ 2 x 10^{-3} M(HQ/Q).

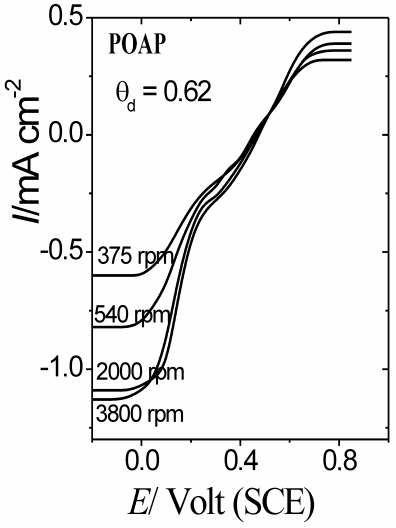

Fig. 4. Steady-state current-potential (*I-E*) curves for different rotation rates (Ω) of the rotating disc electrode. A deactivated POAP film ($\theta_d = 0.62$). Ω values are indicated in the figure. Film thickness: 60 nm. Electrolyte: 0.1 M $HClO_4$ + 0.4 M $NaClO_4$ + 2 x 10^{-3} M(HQ/Q).

variable. $I_{lim,c}$ *versus* $\Omega^{1/2}$ dependences at potential values $E < 0.0$ V for both nondeactivated and deactivated POAP films are shown in Fig. 5. For a nondeactivated POAP film a linear $I_{lim,c}$ *versus* $\Omega^{1/2}$

dependence, which follows the Levich equation, is obtained within a wide range of Ω values (empty circles in Fig. 5). However, for POAP films that have been deactivated by storage without use for different time periods, after a certain Ω value, a constant cathodic limiting current value, $I_{lim,c}$, independent of Ω is achieved (black triangles in Fig. 5). Also, it is observed that the transition at which the cathodic limiting current becomes independent of Ω occurs at lower Ω values as the degree of deactivation increases. The explanation of this effect can be given in terms of the electron hopping model [21, 22]. Limiting current values at which $I_{lim,c}$ (= I_e) becomes constant were considered as a representation of the maximum flux of electrons confined in the polymer, according to Eq. (2) [22]

$$I_e = n\ F\ A\ D_e\ c/\phi_p \qquad (2)$$

In Eq. (2), c is the concentration of redox sites of the polymer and ϕ_p the polymer film thickness. D_e represents a measure of the electron hopping rate and n expresses the numbers (fractions) of unit charges per monomer unit of the polymer. A is the electrode area and F the Faraday's constant. Experimental I_e values, corresponding to each one of the eight deactivated POAP films in contact with a 2 x 10^{-3} M HQ/Q solution, were extracted from the cathodic plateau and they are listed in Table 2 (Third column). As can be seen from Table 2, I_e decreases with increasing θ_d. The constant value of the current (I_e) at a given Ω value for deactivated POAP films can be related to a slow electron transport across the POAP film that mediates in the electron-transfer reaction at the polymer|solution interface, as compared with a nondeactivated POAP film. As one increases the flux of Q (increase of Ω) from the bulk solution, and if the flux exceeds the supply of electrons from the electrode through the polymer to the electrolyte interface, the rate-limiting step will shift from the limiting transport of Q to the limiting transport of the charge through the polymer. In order to verify this limiting charge-transport process across the POAP film, the HQ/Q concentration in solution was varied. It was found that the constant current for a given deactivated film remains unchanged with changing redox couple concentration in solution. According to Eq. (2), the slower electron

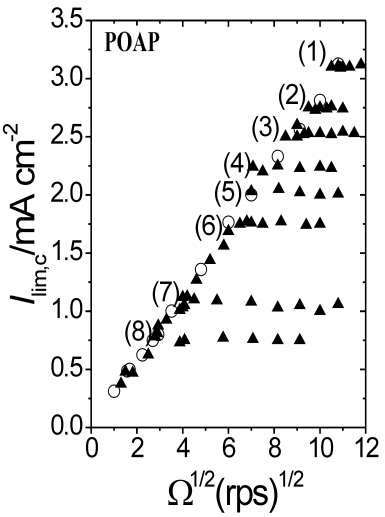

Fig. 5. Levich representations $I_{lim,c}$ *versus* $\Omega^{1/2}$ for POAP films in contact with a 0.1 M $HClO_4$ + 0.4 M $NaClO_4$ + 2 x 10^{-3} M (HQ/Q) solution. (O) Empty circles correspond to a nondeactivated POAP film. Black triangles correspond to deactivated films. Numbers from (1) to (8) indicate the different films listed in Table 1.

Table 2. Efficiency (I_e/I_o x100)) of a POAP film to act as mediator in the HQ/Q redox reaction after storage without use in the supporting electrolyte solution for different time periods.

POAP Film	θ^d	I_e/mA cm^{-2}	I_e/I_o x 100
1	0.05	3.01	94
2	0.10	2.75	86
3	0.15	2.55	79
4	0.25	2.23	70
5	0.35	2.02	63
6	0.41	1.74	54
7	0.62	1.05	33
8	0.77	0,55	16

transport in deactivated films, as compared with nondeactivated ones, could be attributed to a decrease in D_e. By employing the I_e values shown in Table 2 and using the parameter values c = 4.7 M [1], A = 1 cm^2, n = 0.44 [24] and ϕ_p = 60 nm in Eq. (2), one obtains a decrease in D_e from 2.00 x 10^{-11} to 0.5 x 10^{-11} cm^2 s^{-1} for a relative increase of θ_c from 0.05 to 0.77. As can be seen from Fig. 6, the electron diffusion coefficient extracted from RDEV measurements seems to decrease linearly

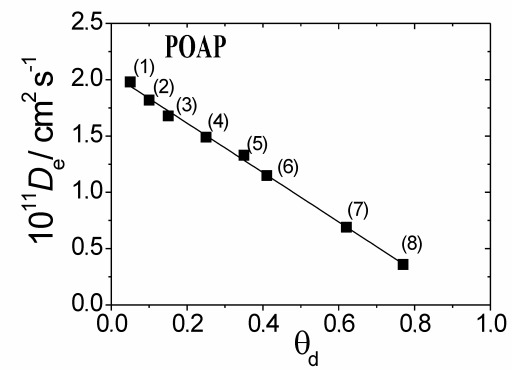

Fig. 6. Electron diffusion coefficient (D_e) (Eq. (2)) as a function of θ_d. Numbers (1) to (8) correspond to each one of the deactivated POAP films listed in Tables 1 and 2.

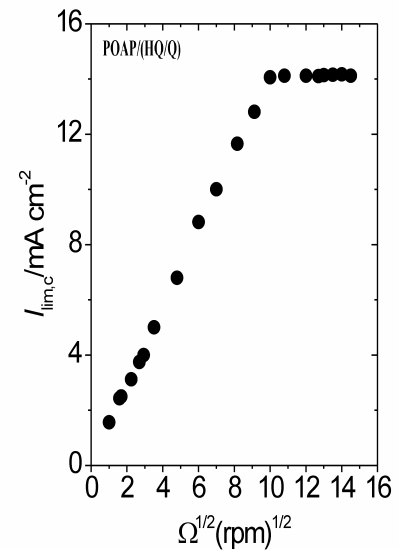

Fig. 7. Levich representation $I_{lim,c}$ *versus* $\Omega^{1/2}$ for a nondeactivated POAP film in contact with a 0.1 M $HClO_4$ + 0.4 M $NaClO_4$ + 0.01 M (HQ/Q) solution.

with the increase in θ_d. The electron diffusion coefficient, D_e, in electroactive materials has been expressed in terms of the mean distance between adjacent active redox sites [25], according to $D_e = (a^2 k_o)$, where k_o is the intermolecular electron-transfer rate constant and a is the mean distance between two adjacent redox sites. The hopping rate, k_o, exhibits an exponential dependence on a, through the energy $-U(x+a)$ of a state with an electron in the position x along the current direction (see Eq. (23) in Ref. [25]). In this respect, a k_o decrease should be expected as the hopping distance a increases. The decrease in D_e obtained from Eq. (2) could be attributed to an increase in the hopping distance between remnant active redox sites after polymer deactivation by storage. As the electronic conductivity in electroactive polymers depends on the electron diffusion coefficient, the D_e decrease with *pH* increase was adjudicated to a decrease in the intermolecular electron-transfer rate constant, k_o, with the polymer deprotonation. In this regard, it is well-known that POAP deactivates with the increase in the solution *pH* [1, 2]. It is interesting to remark that a constant current I_e independent of Ω is also obtained for a nondeactivated POAP film in contact with a 0.1 M $HClO_4$ + 0.4 M $NaClO_4$ + 2 x 10^{-3} M Q/HQ solution. However, in this case the constant current is obtained at very high electrode rotation rates (Ω > 9000 rpm). It is possible that at high angular speeds of the rotating disc electrode, the flux into the bulk solution would not longer be laminar, such that the proportionality between the current and $\Omega^{1/2}$, should not be expected. However, if the HQ/Q concentration is increased (0.01 M) a constant current I_e (≈ 15 mA cm^{-2}) is observed for a nondeactivated film at about 7000 rpm (Fig. 7). As this value is reproducible and it decreases as the deactivation of the polymer increases, our interpretation of a change in the rate limiting process during the mediated electron-transfer reaction seems to be correct. Considering the constant current value obtained for high HQ/Q concentrations, a D_e about 1.22 x 10^{-10} cm^2 s^{-1} is obtained for a nondeactivated POAP film. This finding seems to indicate that a restriction for the electron transport also occurs across a nondeactivated POAP film in contact with a concentrated electroactive solution and high enough flux into the bulk solution. On the basis of data showed in Figs. 5 and 6, one can assess the efficiency of POAP to act as mediator in the 0.1 M $HClO_4$ + 0.4 M $NaClO_4$ + 2 x 10^{-3} M Q/HQ solution. By taking as reference a high enough electrode rotation rate (Ω = 7000 rpm) to reach a constant current for all the deactivated films treated in the work (Figs. 5 and 6), one can calculate the (I_e/I_o x100) ratio, where I_e are the different constant current values for the different deactivated films (see Table 2) and I_o is the current value (3.2 mA cm^{-2}) corresponding to the nondeactivated film, which follows the Levich

relationship at Ω = 7000 rpm (Fig. 5). In Table 2, (I_e/I_o x 100) represents the efficiency of POAP to act as mediator in the HQ/Q redox reaction. For a nondeactivated film, $I_o = I_e$= 3.2 mA cm^{-2} at Ω = 7000 rpm, then, I_e/I_o = 1 and (I_e/I_o x 100) = 100, which corresponds to the maximal efficiency. As can be seen from the Table 2, the efficiency of a POAP film is reduced to about 16 percent for a storage time without use for 120 h.

Impedance measurements were also performed with nondeactivated and deactivated POAP films contacting a 0.1 M $HClO_4$ + 0.4 M $NaClO_4$ + 2 x 10^{-3} M (Q/HQ) solution at potential values E < 0.0 V. Nyquist diagrams at different electrode rotation rates for a nondeactivated POAP film are shown in Fig. 8. A Warburg region at high frequency, followed by a semicircle, is observed in the impedance diagrams of a nondeactivated film. Impedance diagrams of each one of the eight deactivated POAP films indicated in Table 1 exhibit two loops (Fig. 9). While the loop at low frequency is Ω-dependent, the high-frequency semicircle is independent of this variable. However, the size of the high-frequency semicircle depends on the degree of deactivation (Fig. 10). In this regard, at a given Ω value, the higher the θ_d value is, the greater the high-frequency semicircle becomes. Although several *ac* impedance diagrams at potential values within the range -0.30 V < E < 0.0 V (*versus* SCE) were recorded for different POAP films, those shown in Figs. 8 to 10 were considered as representative of the potential region where POAP is in its reduced state. The coverage of the gold disc surface with an evaporated gold film, as described in the 'Materials and Methods' section, leads to reproducible impedance data within the potential range comprised between -0.3 V and 0.0 V. The good reproducibility can be attributed to the use of a smooth and renewable gold surface, obtained

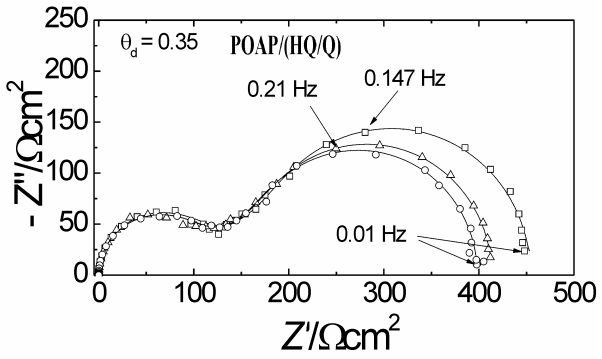

Fig. 9. *Ac* impedance diagrams in the Nyquist coordinates (-*Z*'' *versus Z*) obtained at E = -0.2 V for a deactivated POAP film, θ_d = 0.35. The different diagrams correspond to different electrode rotation rates, Ω : (O) 2600 rpm; (Δ) 1500 rpm ; (□) 1000 rpm. Electrolyte: 0.1 M $HClO_4$ + 0.4 M $NaClO_4$ + 2 x 10^{-3} M (HQ/Q) solution. Discrete points are experimental data and continuous lines represent the theoretical fitting by using Eq. (3).

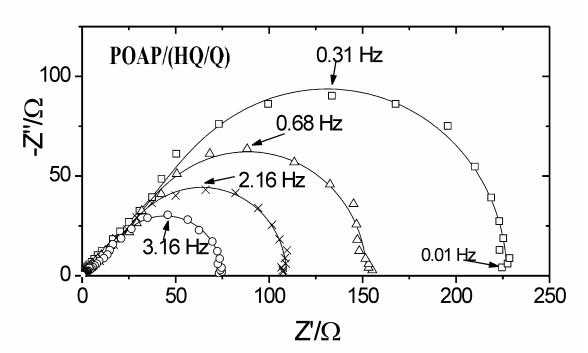

Fig. 8. *Ac* impedance diagrams in the Nyquist coordinates (-*Z*'' *versus Z*) obtained at E = -0.3 V for a nondeactivated POAP film. The different diagrams correspond to different electrode rotation rates, Ω : (□) 100 rpm; (Δ) 200 rpm; (X) 300 rpm; (O) 600 rpm. Electrolyte: 0.1 M $HClO_4$ + 0.4 M $NaClO_4$ + 2 x 10^{-3} M (HQ/Q) solution. Discrete points are experimental data and continuous lines represent the theoretical fitting by using Eq. (3).

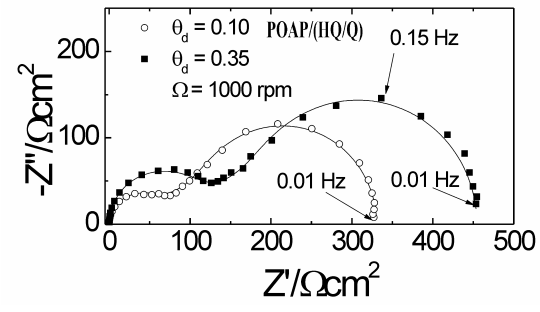

Fig. 10. *Ac* impedance diagrams in the Nyquist coordinates (-*Z*'' *versus Z*) obtained at E = -0.2 V and a constant electrode rotation rate, Ω = 1000 rpm, for two deactivated POAP films: (O) θ_d = 0.10; (■) θ_d = 0.35. Electrolyte: 0.1 M $HClO_4$ + 0.4 M $NaClO_4$ + 2 x 10^{-3} M (HQ/Q) solution. Discrete points are experimental data and continuous lines represent the theoretical fitting by using Eq. (3).

by evaporation, to deposit the POAP film in each experiment. However, it should be indicated that impedance data at potential values slightly more negative than -0.30 V exhibit a strong increase in values of the real impedance constituent, which leads to poor reproducibility of experimental data. In this regard, at potential values more negative than -0.30 V, the gold film deposited by vacuum evaporation on the gold disc electrode is slowly detached (peeled off) from the gold disc surface, possibly due to incipient hydrogen evolution (bubbles on the gold film surface are visible). Impedance data obtained in such conditions were not reproducible, and they are not presented here.

Interpretation of ac impedance diagrams

On the basis of the experimental arrangement used, i.e., a gold disc electrode of low surface roughness (high specularity) after deposition of a thin gold film by evaporation coated with a thick POAP film [7], the system could be considered as a good enough approximation to a uniform polymer layer deposited on a smooth electrode surface to apply a homogeneous electrochemical impedance model in the interpretation of experimental *ac* impedance diagrams.

It is well-known that thin metal films obtained by evaporation (low rate of evaporation) exhibit specular surfaces with a relatively low amount of defects as compared with a massive metal surface. The specularity of a metal film surface is represented by its specularity parameter, p [12]. The value of p for a thin metal film can be interpreted as the fraction of the surface which specularly reflects conduction electrons from the inside of the film to its surface. The value of p ranges from 0 for complete diffuse scattering to 1 for complete specular scattering. The value of p depends on the quality of the metal film surface, that is, on the method of preparation of the metal film. Thus, a metal film surface with a smooth mirror-like finish, which is free of defects, should have a specularity parameter near 1. Our gold films are prepared at low evaporation rates and they show a specularity parameter near 0.91. For more details about the significance of p see 'Electronic transport in thin metal films' section. With regard to the thickness of the POAP film, it was demonstrated in a previous work [23] that POAP deposition on a rotating gold disc starts with the formation of a rather porous structure whereas dense structures are formed later on as the polymer thickness increases. scanning electron microscopy (SEM) images (Fig. 8 in reference [23]) and permeation rate measurements (Table 1 in reference [23]) show that thick POAP films are uniform and compact enough to restrain the physical diffusion of species through the film. Also, recent resistance measurements on POAP-coated gold film electrodes [12] demonstrate that the POAP coverage higher than 0.8 mC cm^{-2} (60 nm) are sufficiently compact at the gold-POAP interface to prevent the specific adsorption of anions and cations proceeding from the external electrolyte solution on the gold film surface. Then, as indicated above, the general theory of *ac* impedance described by Vorotyntsev *et al*. in reference [18] was employed to interpret experimental impedance data of this modified electrode system. It should be indicated that the theory developed in reference [18] is strictly valid when the charging of interfacial double layers is negligible, i.e., it does not account for the charging of the film|substrate and film|solution layers in parallel with the processes of injection of charge carriers. If this is not the case, a more complete model, such as the one developed by Vorotyntsev in other work [26], should have to be used. In this model [26], besides the traditional "double-layer" capacitance and interfacial charge-transfer resistances, two additional parameters for each boundary, "interfacial numbers" for each species and "asymmetry factors," are introduced. Although we also fitted our experimental impedance diagrams with the model reported in reference [26], the fitting was not as good as that using the model given in reference [18], and furthermore, the increasing mathematical difficulty of determining the numerous parameters of the model given in reference [26] from experimental data was a major drawback. Then, despite this last theoretical limitation, the model described in paper [18] concerning a uniform and nonporous film with no penetration of redox species from the solution was employed to interpret our experimental impedance diagrams.

As in the present case one has the modified electrode geometry with a redox active electrolyte solution (m|film|es), Eq. (41) in Ref. [18] (Eq. (3) in this work) must be applied

$$Z_{m|film|es} = R_{m|f} + R_f + R_s + [Z_e^{f|s}\, R_i^{f|s} + W_f\, Z_{12}^{m}] \\ (Z_e^{f|s} + R_i^{f|s} + 2\, W_f\, \coth 2\nu)^{-1} \qquad (3)$$

where

$$Z_{12}^{m} = Z_e^{f|s} [\coth \nu + (t_e - t_i)^2 \tanh \nu] + R_i^{f|s} 4t_i^2 \tanh \nu + W_f 4t_i^2 \quad (4)$$

In Eqs. (3) and (4):

$\nu = [(j\omega\phi_p^2)/4D]^{1/2}$ is a dimensionless function of the frequency ω, ϕ_p is the film thickness, D is the binary electron-ion diffusion coefficient, and t_i and t_e are the migration (high frequency) bulk-film transference numbers for anions and electrons, respectively. D is defined as $D = 2D_iD_e(D_e+D_i)^{-1}$ and $t_{i,e} = D_{i,e}(D_e+D_i)^{-1}$, where D_e and D_i are the diffusion coefficients for the electrons and ion species, respectively.

$W_f = [\nu/j\omega\phi_pC_p] = \Delta R_f/\nu$ is a Warburg impedance for the electron-ion transport inside the polymer film. ΔR_f ($=\phi_p/4DC_p$) is the amplitude of the Warburg impedance inside the film, and C_p is the redox capacitance per unit volume.

$R_f(=\phi_p/\kappa)$ is the high-frequency bulk-film resistance, R_s the ohmic resistance of the bulk solution (κ is the high-frequency bulk conductivity of the film), $R_{m|f}$ is the metal|film interfacial electron-transfer resistance, and $R_i^{f|s}$ is the film|solution interfacial ion-transfer resistance.

$Z_e^{f|s} = (R_e^{f|s}+W_s)$ is the electronic impedance, where $R_e^{f|s}$ is the interfacial electron-transfer resistance at the film|solution interface, and W_s is the convective diffusion impedance of redox species in solution, which contains the bulk concentrations of ox(red) forms, $c_{ox}(c_{red})$, and their diffusion coefficients inside the solution, $D_{ox}(D_{red})$. Also, it contains the Nernst layer thickness, δ.

$R_e^{f|s}$ is defined as

$$R_e^{f|s} = RT\,(nF^2k_oc_{red})^{-1} \quad (5)$$

where k_o is the rate constant of the reaction between the film and the redox active forms in solution. Diffusion of the redox forms from the bulk solution to the film|solution interface can be regarded as stationary through the diffusion layer thickness, expressed in cm by

$$\delta = 4.98\, D_{ox,red}^{1/3}\, \eta^{1/6}\, \Omega^{-1/2} \quad (6)$$

where η is the kinematic viscosity of the solution in the same units as $D_{ox,red}$, and Ω the rotation rate of the disk electrode in rpm. The rest of the constants have their usual meaning. This model also includes the impedance behavior of the polymer in contact with the inactive electrolyte (absence of the redox couple in solution) by considering $Z_e^{f|s} \to \infty$ in Eq. (3).

Dependences of the different charge-transport and charge-transfer parameters on the degree of deactivation

As indicated above, continuous lines on the impedance diagrams shown in Figs. 8 to 10 are simulated curves calculated by using Eq. (3). As it is often considered that some transformed curves could give more valuable information about the goodness of the fitting than Nyquist plots, real and imaginary parts *versus* frequency plots corresponding to each one of the Nyquist representations were also built. One of these representations for a θ_c^d value of 0.42 is shown in Fig. 8. A good fitting was observed for the different impedance diagrams. The fitting procedure by using Eq. (3) was based on the CNLS (Complex Nonlinear Squares) method. A rigorous fitting procedure was performed. Six replicate measurements for each degree of deactivation were carried out, and the error structure was assessed following the method recommended by Agarwal *et al*. [27] and Orazem [28]. The standard deviation for the real (σ_{Zr}) and imaginary (σ_{Zj}) parts of the impedance followed the form proposed by Orazem (see Eq. (8) in Ref. [28])

$$\sigma_{Zr} = \sigma_{Zj} = \alpha\,|Zj| + \beta\,|Zr| + \gamma\,|Z|^2 Rm^{-1} + \delta \quad (7)$$

where Rm is the current measuring resistor used for the experiment, Zr is the real part of the impedance, and Zj is the imaginary part of the impedance. α, β, γ and δ are constants that have to be determined. The values of these scaling factors were $\alpha = 0$, $\beta = 3.15 \times 10^{-3} \pm 0.005 \times 10^{-3}$, $\gamma = 2.7 \times 10^{-5} \pm 0.1 \times 10^{-5}$ and $\delta = 6.8 \times 10^{-3} \pm 0.3 \times 10^{-3}$. The error structure was found to follow the same model within the range of degree of capture $0.05 < \theta_d < 0.77$. At θ_d values lower than 0.05, the error structure model parameters had different values, but these results are not reported here. Then, continuous lines in Figs. 8 to 10 and point representation in Fig. 11 represent the weighted complex nonlinear least-squares fit to the data. The regression was weighted by the inverse of the variance of the stochastic part of the measurement. In all conditions the weighted sum of the square of the residuals was below one [28].

In the simulations the number of transferred electrons, n, was assumed to be 0.44 [24], and diffusion coefficient values of the redox species (Q and HQ) were considered equal, $D_{ox,red}$ = 1.5 x 10^{-5} cm^2 s^{-1}. Also, the bulk concentrations of the redox substrate species were considered equal (c_{ox} = c_{red} = 2 x 10^{-6} mol cm^{-3}). The polymer thickness was considered as ϕ_p = 60 nm. The value of the total redox site concentration of POAP was considered as c_o = 4.7 x 10^{-3} mol cm^{-3} [1]. The ohmic resistance of the solution in contact with the polymer films, R_S, was measured. A value R_S ~ 1.43 ohm cm^2 was obtained. Then, by considering the high-frequency intercept of impedance diagrams of POAP films in the presence and in the absence of the redox couple in solution as R_o, the high-frequency bulk POAP film resistance, R_f, was calculated as $R_f = R_o - R_S$ [29]. The latter value varied within the range 1.17 < R_f < 2.14 ohm cm^2 and it seems not to be strongly dependent on the degree of deactivation. Then, R_f and R_S values were imposed in the fitting. The remnant parameters contained in Eq. (3) ($R_{m|f}$, $R_i^{f|s}$, $R_e^{f|s}$, C_p, D_e and D_i) were calculated from the experimental impedance data by the fitting procedure described above. The first three parameters ($R_{m|f}$, $R_i^{f|s}$ and $R_e^{f|s}$) were varied without restraints during the fitting. However, some reference values were considered for C_p, D_e and D_i. For the nondeactivated POAP film thickness used in this work (ϕ_p = 60 nm) and solution pH = 1, D_e and D_i values were allowed to vary within the range 10^{-7}-10^{-12} cm^2 s^{-1}, in such a way that diffusion coefficient values lower than 10^{-12} were considered unrealistic for these thick films. That is, D_e and D_i values lower than 10^{-12} were only obtained from impedance diagrams (not shown) of very thin POAP films ($Q_{T,Red}$ = 0.15 mC cm^{-2}, ϕ_p = 9 nm) in contact with solutions of pH = 1, where incomplete coating of the metal area by the thin polymer film is possible. Concerning C_p, reference values were extracted from experimental -Z" *versus* ω^{-1} slopes of impedance diagrams at sufficiently low frequency (in the absence of the redox substrate in solution). A contribution of the interfacial capacitance, C_H, also considered as a fitting parameter, was included in order to represent the actual impedance diagrams from the calculated ones.

Different charge-transport and charge-transfer parameters versus θ_d dependences, extracted from the fitting procedure described above, are shown in Figs. 12 to 17. The C_p versus θ_c dependence is shown in Fig. 12. As can be seen, starting from a C_p value of about 27.5 F cm^{-3}, for a nondeactivated film, a slow decrease in C_p with increasing θ_d up to 0.3 is observed. Then, from a degree of deactivation of 0.3 up to 0.77, a more pronounced decrease is observed. In this regard, a break at a degree of deactivation about 0.3 seems to be evident in the C_p versus θ_c dependence. The observed decrease in the redox capacitance is consistent with the gradual attenuation of the voltammetric response

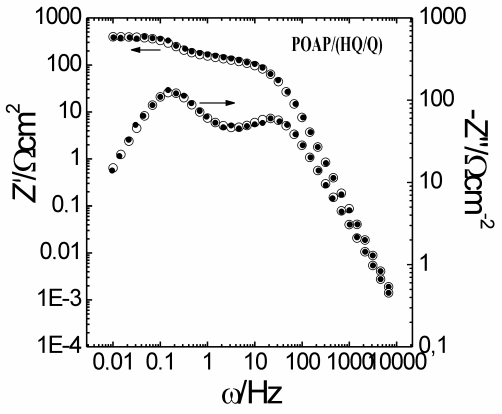

Fig. 11. Real part (Z') and imaginary part (-Z") *versus* frequency (ω) plots (point-to-point representations) for a POAP film with θ_d = 0.62. E = -0.3 V, Ω = 2600 rpm. Electrolyte: 0.1 M $HClO_4$ + 0.4 M $NaClO_4$ + 2 x 10^{-3} M (HQ/Q) solution. (•) Experimental data; (O) fitting employing Eq. (3).

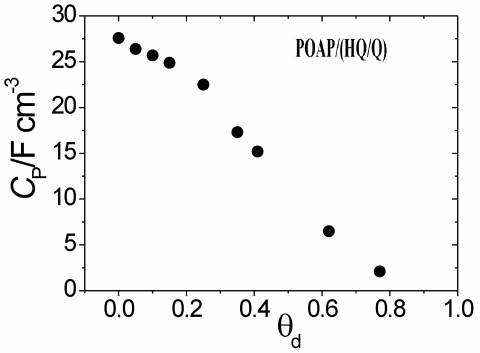

Fig. 12. Redox capacitance (C_p) as a function of θ_d. The value 27.5 F cm^{-3} for θ_d = 0 corresponds to a nondeactivated film. Electrolyte: 0.1 M $HClO_4$ + 0.4 M $NaClO_4$ + 2 x 10^{-3} M (HQ/Q) solution.

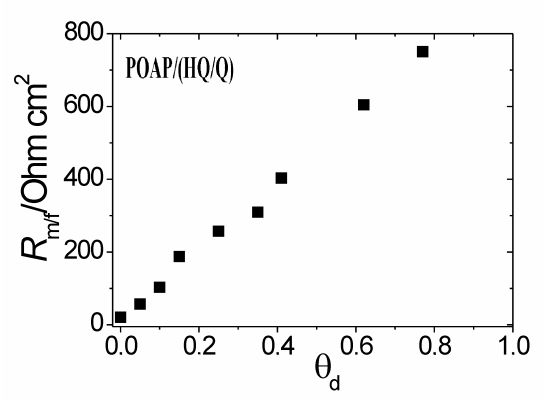

Fig. 13. Metal-polymer interfacial electron-transfer resistance ($R_{m/f}$) as a function of θ_d. Electrolyte: 0.1 M $HClO_4$ + 0.4 M $NaClO_4$ + 2 x 10^{-3} M (HQ/Q) solution.

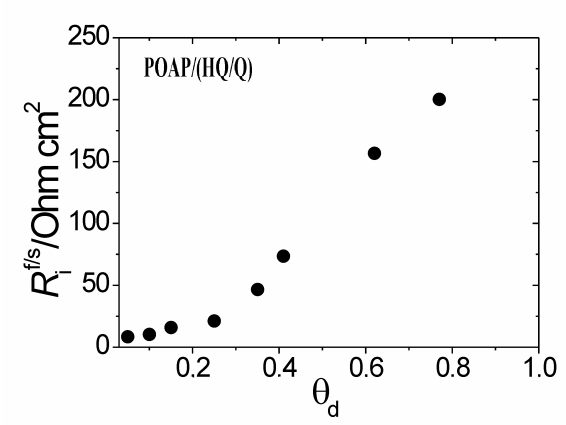

Fig. 14. Polymer-solution interfacial ion-transfer resistance ($R_i^{f/s}$) as a function of θ_d. Electrolyte: 0.1 M $HClO_4$ + 0.4 M $NaClO_4$ + 2 x 10^{-3} M (HQ/Q) solution.

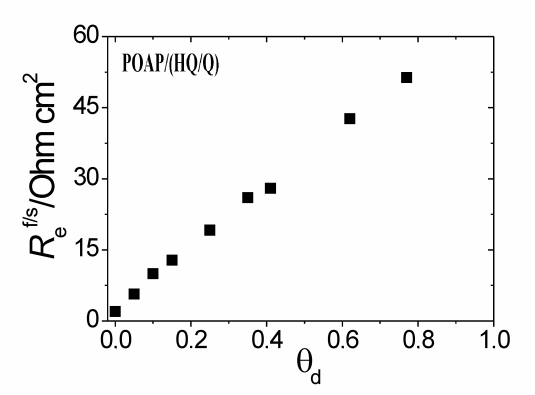

Fig. 15. Interfacial electron-transfer resistance ($R_e^{f/s}$) as a function of θ_d. Electrolyte: 0.1 M $HClO_4$ + 0.4 M $NaClO_4$ + 2 x 10^{-3} M (HQ/Q) solution.

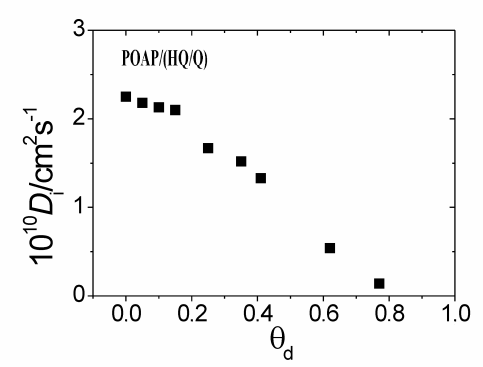

Fig. 16. Ion diffusion coefficient (D_i) as a function of θ_d. Electrolyte: 0.1 M $HClO_4$ + 0.4 M $NaClO_4$ + 2 x 10^{-3} M (HQ/Q) solution.

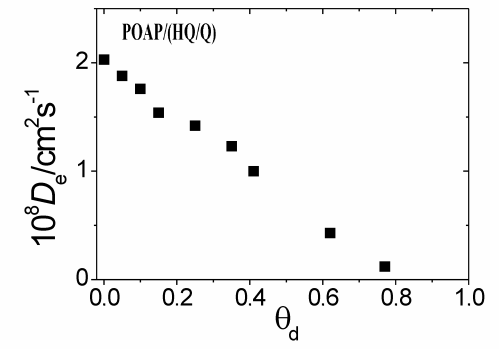

Fig. 17. Electron diffusion coefficient (D_e) as a function of θ_d. Electrolyte: 0.1 M $HClO_4$ + 0.4 M $NaClO_4$ + 2 x 10^{-3} M (HQ/Q) solution.

as the degree of deactivation increases (Fig. 1). It should be kept in mind that these C_p values correspond to the reduced state of POAP. There was no difference in the redox capacitance *versus* θ_d dependence achieved in the supporting electrolyte from the -*Z*'' *versus* ω^{-1} slopes and in the presence of the redox active substrate from Eq. (3). Only small differences in the numerical values of C_p were found. The good agreement between the redox capacitance values attained under these different conditions could be considered as an indication of the high fitting accuracy reached to obtain optimum parameter values (in this case C_p) for the treated system by using Eq. (3). $R_{m|f}$ and $R_i^{f|s}$ on θ_d dependences are shown in Figs. 13 and 14, respectively. $R_i^{f|s}$ as a function of θ_d exhibits a different feature as compared with $R_{m|f}$. That is, while $R_{m|f}$ increases almost linearly within the whole

θ_d range, $R_i^{f|s}$ shows a clear break about a degree of deactivation of 0.3. In this regard, $R_i^{f|s}$ firstly exhibits a slow increase in the θ_d range comprised between 0.0 and 0.3 and then, a more pronounced increase between 0.3 and 0.7 is observed. The magnitudes of $R_{m|f}$ and $R_i^{f|s}$ within the whole θ_c^d range are also different. The whole $R_i^{f|s}$ change is around four times lower than $R_{m|f}$ change. It is possible that both resistances contribute to the high-frequency semicircle on impedance diagrams shown in Figs. 8 to 10. The increase in interfacial $R_{m|f}$ resistance could be due to an increasing number of inactive sites at the metal|polymer interface with the increase in deactivation. The $R_i^{f|s}$ increase with the increase in the degree of deactivation could be attributed to an increasing difficulty to incorporate ions into the polymer matrix as the polymer becomes more deactivated. $R_e^{f|s}$ values were extracted from Eq. (5) using k_o as fitting parameter ($0.01 < k_o < 1000$ cm s^{-1}). The feature of $R_e^{f/s}$ *versus* θ_d dependence is similar to $R_{m/f}$ *versus* θ_d dependence. However, the $R_e^{f|s}$ values are around one order of magnitude lower than $R_{m/f}$ values. Also, it is interesting to note that the $R_e^{f|s}$ change is lower than the $R_i^{f|s}$ change within the whole θ_d range. Then, the storage time without use seems to affect more strongly the polymer|solution interfacial ion-transfer resistance $R_i^{f|s}$ than the polymer|solution interfacial electron-transfer resistance, $R_e^{f|s}$. The increase in interfacial $R_e^{f|s}$ resistance could be due to an increasing number of inactive sites at the polymer|solution interface with the increase in deactivation. Ion and electron diffusion coefficients *versus* θ_d dependences are shown in Figs. 16 and 17, respectively. Both diffusion coefficients decrease as θ_d increases. However, while D_e decreases almost linearly with the increase in θ_d, D_i *versus* θ_d exhibits a break at about $\theta_d = 0.3$. Also, D_e values are nearly two orders of magnitude higher than D_i values. It is possible that electron hopping controls the charge-transport process at a POAP film in its oxidized state, where the polymer is swollen, which facilitates ion transport. However, in the present work, relative diffusion coefficient values ($D_e > D_i$) refer to the reduced state of POAP. As was above proposed from RDEV data, the decrease in D_e with the increase in θ_d could be attributed to an increase in the hopping distance between remnant redox active sites after polymer deactivation. Although the Vorotyntsev's model gives D_e values near three orders of magnitude higher than D_e values extracted from RDEV, both D_e *versus* θ_d dependences are linear. The interpretation of diffusion coefficients at polymer films depends on the model employed to describe the charge propagation and sometimes on the technique used in its measurement. The break observed in the D_i *versus* θ_d dependence at about $\theta_d \sim 0.3$ also seems to be evident in the $R_i^{f|s}$ *versus* θ_d dependence (Fig. 14). Probe beam deflection measurements [30] suggest that while protons and anions are exchanged during POAP oxidation, insertion of protons is the dominant process during the POAP reduction process. Also, impedance measurements reported in reference [7] indicate that POAP is only doped with hydrogen ions and the effect of anions is negligible. Then, it is possible that both parameters $R_i^{f|s}$ and D_i are related to proton movements across the POAP|solution interface and inside the polymer film, respectively, rather than to anion transport. Concerning the proton movement into POAP films, the existence of two forms (mobile and bound) of hydrogen ions in the bulk film has been proposed in reference [7]. It was suggested that in polymers derived from aromatic amines, hydrogen ions could be constrained by nitrogen atoms of polymer chains and do not contribute to the electrical conductance of the film, and another part of such constrained groups is able to dissociate producing the mobile form of hydrogen, which provides the film conductance. In other words, besides mobile protons, some traps for hydrogen ions within the bulk of the film may be present, which provides the binding of these protons with polymer film fragments. This proton conduction mechanism is similar to that proposed for ion transport in some solid-state materials [31], where ion movement occurs by a hopping process with the participation of two different types of sites. While some sites allow a fast ion diffusion process, other sites immobilize ions and do not allow ions to participate in the diffusion process. The existence of these different types of sites was explained in terms of different energy barriers [31]. In this regard, the slight increase in the $R_i^{f|s}$ *versus* θ_d (the slight decrease in the D_i *versus* θ_d) dependence within the range $0 < \theta_d < 0.3$ could be due to the inhibition of traps for hydrogen ions, which only causes a small ion conductivity change. However, the strong $R_i^{f|s}$ increase (more pronounced D_i decrease) for

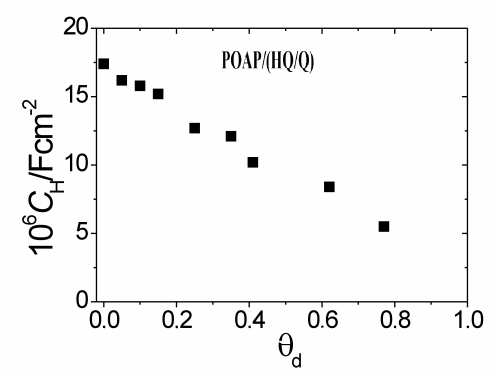

Fig. 18. Interfacial capacitance C_H at the metal-polymer interface as a function of θ_d. Electrolyte: 0.1 M $HClO_4$ + 0.4 M $NaClO_4$ + 2 x 10^{-3} M (HQ/Q) solution.

$\theta_d > 0.3$ could be attributed to the inhibition of nitrogen-containing groups that provide the binding of hydrogen ions and at the same time are able to dissociate and give the mobile form of hydrogen that markedly contributes to the polymer conductivity. With regard to C_H values, starting from a value of around 17.5 μF cm^{-2} for a nondeactivated film, C_H decreases almost linearly as the degree of deactivation increases, reaching a value of about 5.5 μF cm^{-2} for $\theta_d \sim 0.77$ (Fig. 18). The C_H decrease, in the same way as the $R_{m|f}$ increase, could be assigned to the creation of inactive gaps in the redox site configuration at the polymer|metal interface with deactivation.

Impedance measurements in the sole presence of the supporting electrolyte

As indicated above, the model of Vorotyntsev *et al*. [18] also includes the impedance behavior of the polymer in contact with the inactive electrolyte (absence of the redox couple in solution) by considering $Z_e^{f|s} \rightarrow \infty$ in Eq. (3). Charge transport and transfer parameters in the absence of the HQ/Q redox couple in solution were also obtained by fitting impedance diagrams in the sole presence of the supporting electrolyte by employing the model described in reference [18]. Impedance parameters not related to the presence of the redox couple in solution obtained by employing Eq. (3) are in coincidence with those extracted in the sole presence of the supporting electrolyte. However, it is often remarked that charge-transport parameter values extracted from impedance measurements depend on the model used to describe the charge propagation in electroactive materials. In this regard, the rate of charge transport in electroactive polymers is usually characterized by diffusion coefficient values, which can vary over several orders of magnitude (10^{-7}-10^{-14} cm^2 s^{-1}). The aim of this part of the work was to study the charge conduction process at POAP films employing a different impedance model to that described by Vorotyntsev *et al*. in reference [18] and then, compare charge-transport parameters obtained from both models. As the electroactivity of POAP is explained by a redox mechanism that involves an addition/elimination of protons coupled with a reversible electron transfer [6], a modified electron hopping model, which considers a protonation reaction, developed by us in reference [32] was used to obtain charge-transport parameters of nondeactivted and deactivated POAP films in the sole presence of the supporting electrolyte solution. Although the model described in reference [32] is more limited than that described in reference [18], the charge-transport parameters obtained from both models were compared. As indicated above, the model given in reference [32] considers a protonation reaction (Reaction (I) see below) coupled with a self-exchange process between oxidized and reduced sites (Reaction II, see below)

$$O + [H^+]_{film} \underset{k'_{-1}}{\overset{k'_1}{\leftrightarrow}} HO^+ \qquad (I)$$

$$OH^+ + e^- \underset{k_b}{\overset{k_f}{\leftrightarrow}} RH \qquad (II)$$

The analytical expression for the impedance derived in a previous work [32] is

$$Z(\omega) = R_{Qt} + (RT/nF^2Ac)\,[k_f + k_b\,(K+1)/K]\; A(\omega, D_e, k) \qquad (8)$$

R_{Qt} in Eq. (8) is a charge-transfer resistance (see also Eq. (32) in reference [32]), which is given by the expression

$$R_{Qt} = (RT/nF^2Ac)\,[(k_f + k_b)\,(k_f\,k_b)^{-1} + 1/K\,k_f] \qquad (9)$$

In Eqs. (8) and (9), A is the electrode area, c the volumetric redox site concentration, and K an equilibrium constant that can be explicitly written in terms of the solution pH as

$$K = (k'_1/k'_{-1})\,K_p\,10^{-pH} \qquad (10)$$

K also depends on the k'_1 and k'_{-1} constants involved in step (I) and on the partition coefficient K_p, which determines the ratio between the proton concentration inside the film ($[H^+]_{film}$) and the actual proton concentration in solution ($[H^+]_{sol}$), i.e.,

$$[H^+]_{film} = K_p\,[H^+]_{sol} \quad (11)$$

k_f and k_b in Eq. (8) are the forward and backward electrochemical rate constants involved in step (II), respectively, and $A(\omega,D_e,k)$ is a function of the frequency, ω, which also contains an affective diffusion coefficient (D_e) to describe the charge-transport process within the polymer film and the constant $k = k'_{-1} + [H^+]_{film}\,k'_1$ (see Eq. (33) in Ref. [32]). OH^+ and RH (steps I and II) are the protonated oxidized and reduced forms of the polymer confined redox couple, respectively. Other chemical equilibria following the self-exchange (II) were ignored in paper [32]. Concerning step (II), the electroactive centers OH^+ and RH can exchange electrons with the electrode at the metal|polymer interface following a Buttler-Volmer kinetics, with k_f and k_b given by the expressions

$$k_f = k_{sh} \exp\,[b_f\,(E-E^o)] \quad (12)$$

$$k_b = k_{sh} \exp\,[-b_b\,(E-E^o)] \quad (13)$$

E^o in expressions (12) and (13) is the standard potential of the redox couple, b_f and b_b are the Tafel coefficients, $b_f = \alpha nF/RT$ and $b_b = (1-\alpha)\,nF/RT$, and k_{sh} is the electrochemical standard rate constant. The other constants have their usual meanings.

The redox centers are uniformly distributed throughout the polymer with a total concentration, c, given by

$$c = [O] + [HO^+] + [RH] \quad (14)$$

Eq. (8) was employed to fit experimental impedance diagrams of nondeactivated and deactivated POAP films in the presence of the supporting electrolyte. Deactivation by storage times was considered to only affect the charge-transfer process at the metal|polymer interface (R_{Qt}) and the charge-diffusion process (D_e) within the polymer film. As the solution pH and electrolyte composition remain constant, the other parameters of the model were assumed to be independent of the deactivation process, and values for nondeactivated POAP films obtained in reference [32] were employed.

Nyquist diagrams at the reduced state (E = -0.2 V) for a nondeactivated POAP film and deactivated films in contact with a 0.1 M $HClO_4$ + 0.4 M $NaClO_4$ solution, are compared in Fig. 19 (see discrete points). The early increase in the imaginary component of the impedance and the absence of any semicircle at high frequency for a nondeactivated film are indicative of a fast interfacial charge-transfer process. However, a well-defined high-frequency semicircle is observed in the impedance diagrams of POAP films stored for prolonged time periods. As the storage time increases, the high-frequency semicircle is more pronounced. As indicated above, the increase in the size of the high-frequency semicircle in Nyquist plots is indicative of a restriction in the charge-propagation process across the gold/POAP/solution system. Continuous lines on the Nyquist plots shown in Fig. 19 are simulated curves calculated by using Eq. (8). A good fitting was observed for all impedance diagrams. In the same way as in the previous model, the fitting procedure by using Eq. (8) was based on the CNLS (Complex Nonlinear Squares) method. A rigorous fitting procedure was performed where the error structure was assessed following the references [27, 28]. Continuous lines in Fig. 19 represent the weighted complex nonlinear least-squares fit to the data.

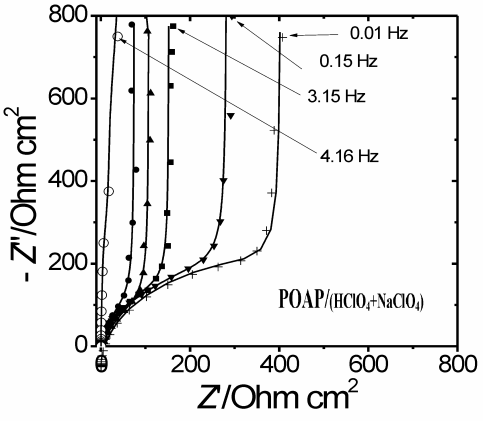

Fig. 19. Nyquist diagrams for (O) a nondeactivated POAP film and for the deactivated films θ_d: 0.05 (•); 0.10 (▲); 0.15 (■); 0.35 (▼); 0.41 (+). E = -0.2 V. Discrete points are experimental data and continuous lines represent the fitting by using Eq. (8). Electrolyte: 0.1 M $HClO_4$ + 0.4 M $NaClO_4$. Thickness of the POAP film: 60 nm.

In the simulations the same parameter values above indicated for the Vorotyntsev model were employed, that is, the number of transferred electrons, n (= 0.44 [24]); polymer thickness, ϕ_p (= 60 nm); total redox site concentration, c (= 4.7 x 10^{-3} mol cm^{-3}); E^o (= 0.015 V *versus* SCE); K (= 0.085 for pH 1) and k (= 0.18 s^{-1}). Then, the remnant—parameters contained in Eq. (8), i.e., k_{sh} and D_e, were calculated from experimental impedance data by the fitting procedure described above. Although the parameter k_{sh} varied without restraints during the fitting, for POAP film thickness (ϕ_p = 60 nm) and solution pH = 1, used in this work, D_e was allowed to vary within the range 10^{-7}–10^{-11} cm^2 s^{-1}. D_e values lower than 10^{-11} cm^2 s^{-1} were considered unrealistic for thick POAP films. A contribution of the interfacial capacitance, C_H, considered as a fitting parameter, was included in order to represent the actual impedance diagrams from the calculated ones. The dependence of the electrochemical standard rate constant (k_{sh}) on the degree of deactivation extracted from the fitting procedure is shown in Table 3. As can be seen from Table 3, k_{sh} decreases as the POAP film becomes more deactivated with the storage time. Similar k_{sh} values for deactivated POAP films shown in Table 3 were previously reported for POAP in reference [24]. In this regard, low values of k_{sh} reported in a previous work could indicate partial deactivation of the polymer. However, high k_{sh} values (2.7 x 10^5 cm s^{-1}) such as that obtained in this work from impedance diagrams for a nondeactivated film (see notes at the foot of Table 3), which do not show an appreciable high-frequency semicircle (Fig. 19), should correspond to a polymer matrix relatively free of deactivated zones. The R_{Qt} *versus* θ_d dependence, extracted from k_{sh} values given in Table 3, is represented in Fig. 20. As can be seen by comparing Fig. 20 with Fig. 13, the R_{Qt} *versus* θ_d dependence extracted from the model given in reference [32] is in good coincidence with the $R_{m/f}$ *versus* θ_d dependence obtained from the model described in reference [18]. As indicated above, although electron hopping is believed to be a mechanism for electron transport at polymer materials, it is also possible that ion motions may partially or totally control the rate of charge transport. Then, D_e obtained with the model derived in reference [32] can be considered as an effective or binary diffusion coefficient value. As can be seen by

Table 3. Standard electrochemical rate constant values for deactivated POAP films. Values extracted from Eq. (8).

[a]POAP films	[b]$10^5 k_{sh}$/cm s^{-1}	[c]θ_d
1	10.5	0.05
2	3.09	0.10
3	3.11	0.15
4	2.04	0.25
5	1,97	0.35
6	1.48	0.41
7	0.67	0.62
8	0.46	0.77

[a]: Numbers 1 to 8 represent different deactivated POAP films.
[b]: Values of the standard electrochemical rate constant, k_{sh}, for the different degrees of deactivation given in column 3. The value of k_{sh} for a nondeactivated film extracted from the fitting using Eq. (8) is 2.7 x 10^5 cm s^{-1}.
[c]: Degree of deactivation of each one of the POAP films after storage for the time periods indicated in column 2 of Table 1. The degree of deactivation was calculated from $\theta_d = 1 - (Q_{Red,c}/Q_{Red,T})$, where $Q_{Red,T}$ (= 2.8 mC cm^{-2}) is the voltammetric reduction charge of a nondeactivated film.

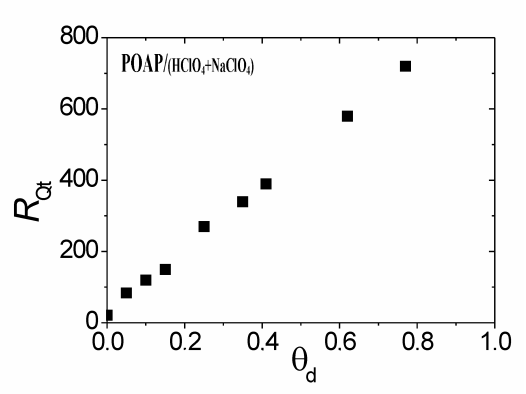

Fig. 20. R_{Qt} *versus* θ_d dependence obtained by employing Eq. (9). Electrolyte: 0.1 M $HClO_4$ + 0.4 M $NaClO_4$ + 2 x 10^{-3} M (HQ/Q) solution.

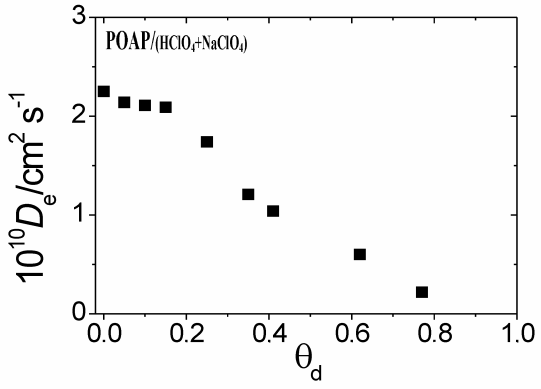

Fig. 21. Diffusion coefficient D_e *versus* θ_d dependence obtained from Eq. (8). Electrolyte: 0.1 M $HClO_4$ + 0.4 M $NaClO_4$ + 2 x 10^{-3} M (HQ/Q) solution.

comparing D_e *versus* θ_d dependence extracted employing the model described in paper [32] (Fig. 21) and D_i and D_e values extracted from Vorotyntsev´s model (Figs. 16 and 17, respectively), the order of magnitude of D_e obtained from the model developed in the pervious work [32] is closer to that of D_i than to that of D_e extracted from the model given in reference [18]. This observation seems to be consistent with the assumption that ion transport controls the whole charge-transport process at POAP. However, D_e values obtained from the impedance model given in reference [32] again are one order of magnitude higher than D_e values extracted from RDEV. The storage without use for prolonged time periods could alter the molecular structure of a POAP film, and, hence, its physical properties. Thus, parameters obtained in this work from impedance models strictly represent fitting parameters of the model rather than real physical properties of the polymer. Even though one cannot expect a complete coincidence of the electrochemical properties of the polymer film with those predicted by the theory, a qualitative agreement might be expected, especially in order to compare the behaviors of films before and after they have been stored for prolonged time periods.

Effect of different deactivation procedures on the charge-transport parameters of POAP films

Dependences of charge-transport and charge-transfer parameters on the degree of deactivation of POAP films obtained in this work were compared with those obtained in other works for POAP films subjected to prolonged electrode potential cycling (PPC) [14], high positive potential limit (HPPL) [15], and soaking in a ferric ion solution (SFeIS) [16].

Fig. 22 compares the electron diffusion coefficient D_e *versus* degree of deactivation θ_d dependences extracted from EIS for the different deactivation processes of POAP. As can be seen by comparing the four D_e *versus* θ_d dependences shown in Fig. 22 (STWU) with those obtained from RDEV data (see Fig. 6), although diffusion coefficient values obtained from the Vorotyntsev *et al.*'s model are three orders of magnitude higher than those obtained from RDEV, the same sequence of D_e values is obtained from both techniques, that is, at each θ_d value D_e (STWU) > D_e (PPC) > D_e (SFeIS) > D_e (HEPP). The consistence of the electron diffusion coefficient sequences obtained from EIS and RDEV measurements could allow one to interpret the rate of electron transport extracted from EIS in terms of different redox site distributions according to the deactivation procedure employed. In this regard again, the more spread redox site distribution should correspond to a POAP film deactivated by applying HPPL as compared with the other deactivation procedures. The comparison of the other charge-transport and charge-transfer parameters *versus* θ_d dependences for the different deactivation processes of POAP is shown in Figs. 23 to 27.

By comparing Figs. 23 and 24, it is interesting to note that $R_{m|f}$ and $R_e^{f/s}$ resistances follow the same

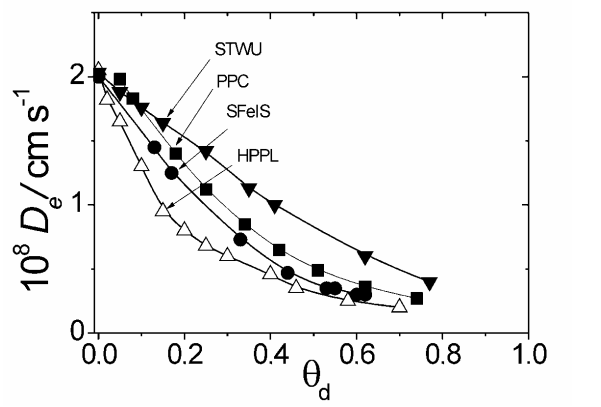

Fig. 22. Comparison of electron diffusion coefficient D_e *versus* θ_d dependence for different deactivation processes of POAP extracted from EIS. Electrolyte: 0.1 M $HClO_4$ + 0.4 M $NaClO_4$ + 2 x 10^{-3} M (HQ/Q) solution. Symbols: (▼) STWU; (■) prolonged potential cycling; (•) soaking in a ferric ion solution and (Δ) high electrode positive potentials. Reduced state of POAP, E = -0.2 V.

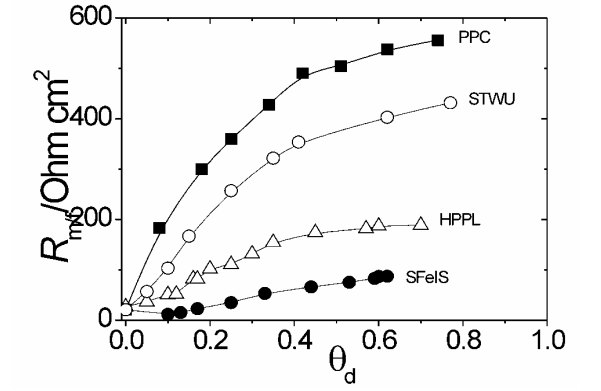

Fig. 23. Metal-polymer interfacial electron-transfer resistance ($R_{m/f}$) as a function of θ_d for the different deactivation processes. Electrolyte: 0.1 M $HClO_4$ + 0.4 M $NaClO_4$ + 2 x 10^{-3} M (HQ/Q) solution.

sequence for the different deactivation processes. That is, while the stronger increase is observed for POAP films subjected to PPC, the interaction with a ferric ion solution causes the lower effect on the electron transfers across the metal|polymer and polymer|solution interfaces. The effects of STWU and HPPL seem to be intermediate between those caused by PPC and SFeIS. As indicated above, $R_i^{f/s}$ and D_i at POAP seem to be related to proton transfer across the polymer|solution interface and proton diffusion across the film, respectively.

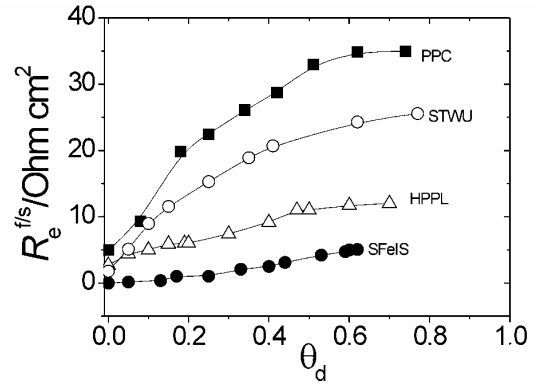

Fig. 24. Interfacial electron-transfer resistance ($R_e^{f/s}$) as a function of θ_d for the different deactivation processes. Electrolyte: 0.1 M $HClO_4$ + 0.4 M $NaClO_4$ + 2 x 10^{-3} M (HQ/Q) solution.

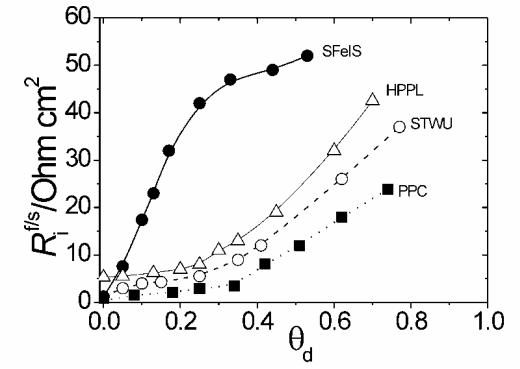

Fig. 25. Polymer-solution interfacial ion-transfer resistance ($R_i^{f/s}$) as a function of θ_d for the different deactivation processes. Electrolyte: 0.1 M $HClO_4$ + 0.4 M $NaClO_4$ + 2 x 10^{-3} M (HQ/Q) solution.

The sequence followed by the polymer-solution interfacial ion-transfer resistance $R_i^{f/s}$ as a function of θ_d (Fig. 25) for the different deactivation processes is opposite to those followed by $R_{m|f}$ and $R_e^{f/s}$. In this regard, the stronger restriction (higher $R_i^{f/s}$ value) for the proton transfer at the polymer|solution interface seems to be caused by the interaction of ferric ions with POAP. Also, as can be seen from Fig. 26, although D_i as a function of θ_d for the different deactivation processes does not follow the same sequence as $R_i^{f/s}$ *versus* θ_d, the incorporation of ferric ions into the POAP matrix causes a more pronounced decrease in the ion diffusion coefficient value as

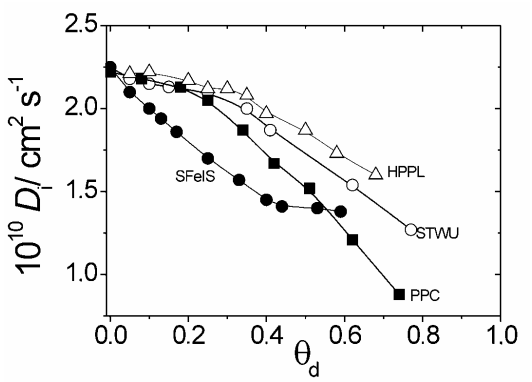

Fig. 26. Ion diffusion coefficient (D_i) as a function of θ_d for the different deactivation processes. Electrolyte: 0.1 M $HClO_4$ + 0.4 M $NaClO_4$ + 2 x 10^{-3} M (HQ/Q) solution.

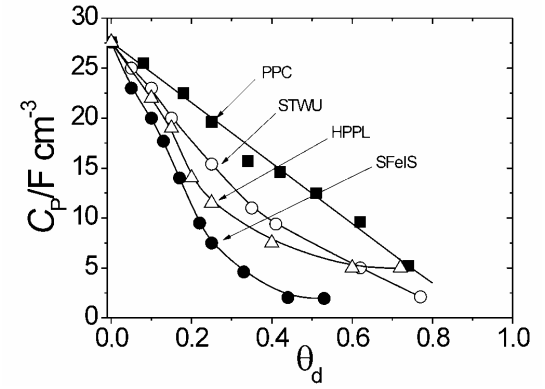

Fig. 27. Redox capacitance (C_p) as a function of θ_d for the different deactivation processes. Electrolyte: 0.1 M $HClO_4$ + 0.4 M $NaClO_4$ + 2 x 10^{-3} M (HQ/Q) solution.

compared with the other deactivation procedures. Thus, soaking of POAP in a ferric ion solution seems to mainly affect the proton diffusion across the film and the proton transfer across the POAP|solution interface. In this regard, deactivation of POAP by SFeIS has been attributed to the direct interaction of iron ions with the redox sites of POAP, which impedes the protonation reaction of the polymer. The redox capacitance (Fig. 27) seems to be strongly affected by the incorporation of iron ions into the POAP matrix. The PPC affects this impedance quantity to a lesser extent. STWU and HPPL seem to cause intermediate effects on the redox capacitance. The same characteristics are observed in the $R_i^{f/s}$ *versus* θ_d dependence (Fig. 25).

Interpretation of surface resistance measurements

Although charge-transport parameters of electroactive polymers are usually obtained employing traditional techniques such as, CV, RDEV and EIS, some experiments employing a non-traditional technique, the surface resistance (SR), were carried out in order to study the POAP deactivation after storage. It is interesting to remark that conversely to other techniques, such as EIS, which is based on complicated models, the SR technique is based on a simple electron dispersion model [33, 34]. The SR technique is sensitive to the distribution of scatterers at a metal film surface [12]. In previous works it was proved that SR is a useful technique to detect changes in the redox sites distribution during the redox switching of a POAP film deposited on a thin gold film [13, 35]. However, as the SR technique may be considered as a non-traditional approach in Electrochemistry, a brief explanation about the interpretation of the resistance changes exhibited by a thin metal film coated with an electroactive polymer film is given in the next paragraphs.

Electronic transport in thin metal films

Electronic transport in thin metal films is strongly affected by interfacial phenomena. For example, the scattering of conduction electrons at planar interfaces defined by the top and bottom surfaces of the film under study can contribute significantly to the resistivity. In the case of thin metal films, the electrical resistivity ρ_f is higher than the bulk resistivity ρ_m of the massive metal of the same structure as the metal film and the ρ_f/ρ_m ratio decreases with increase in the film thickness, ϕ_m. This "Size Effect" becomes evident when ϕ_m is comparable with the mean free path, l_m, of the conduction electrons. The theory to account for the size effect was postulated by Fuchs [33] and Sondheimer [34]. The exact expression for the dependence of the film resistivity, ρ_f, as a function of ϕ_m is complicated. However, it can be reduced to a limiting form when $\phi_m/l_m \geq 1$:

$$\rho_f/\rho_m = 1 + (3/8)\,(1-p)\,l_m/\phi_m \qquad (15)$$

In Eq. (15), p is the specularity parameter [34]. This parameter represents the probability of an electron being reflected specularly or diffusely at the film surface. The p value ranges from 0 for complete diffuse scattering to 1 for complete specular scattering. At first, it should be considered that thin metal films can be prepared to satisfy the Fuch's model in a sufficient way to exhibit a specularity parameter near 1 (a surface with a smooth mirror-like finish which is free of defects). However, this parameter, which is also interpreted as the fraction of the surface which specularly reflects electrons, depends on the quality of the metal film surface, that is, on the method of preparation of the metal film [12]. In this sense, an appreciable fraction of the conduction electrons can be scattered diffusely to give rise to an additional resistance, which correlates with roughness of surface topography and the presence of surface defects. All these imperfections should lead to experimental p values lower than 1.

Besides factors above mentioned if foreign entities are present on the film surface, translational symmetry parallel to the interface, changes and additional scattering of the conduction electrons occurs. This electron dispersion effect brought about by the presence of entities on the metal surface, thereby acting as dispersion centres for the surface reflection of the electrons from the inside of the metal, has been analysed on the basis of Eq. (15). Assuming that the specularity, p, is the principal parameter influenced by the surface concentration of foreign scattering centres at the film surface Γ_{surf}, differentiation of Eq. (15) leads to the relationship:

$$\Delta\rho_f = -\,3/8\,(\rho_m\, l_m/\phi_m)\,(\Delta p) \qquad (16)$$

On the assumption that the increase in Γ_{Surf} increases the diffuse scattering of the electrons, $\Delta p = -\,k\,\Gamma_{Surf}$, an increase in $\Delta\rho_f$ would be expected with increasing Γ_{surf} (Eq. (16)). In terms of the resistance changes ($\Delta R = \Delta\rho_f\, G/\phi_m$), Eq. (16) can be written as:

$$\Delta R = -3/8\; G\,(\rho_m\, l_m/\phi^2_m)\,\Delta p \qquad (17)$$

The POAP-coated gold film electrode

As was described in the 'Materials and Methods' section, POAP was deposited on a thin gold film electrode whose thickness was of the order of the mean free path of conduction electrons of gold, and SR was employed to investigate changes in the electronic properties at the gold|POAP interface during deactivation of the polymer. Simultaneous voltammetric and SR responses corresponding to a nondeactivated POAP film within the potential range comprised between -0.2 V and 0.5 V are shown in Fig. 28.

As indicated above, the POAP film maintains these responses even after storage without use for a time period of 30 h. However, after a higher storage time these responses start to change. The evolution of the $\Delta R/R$ vs. E response for a 60 nm thick POAP film with the storage time is shown in Fig. 29. Simultaneously with the $\Delta R/R$ vs. E response, the evolution of the voltammatric response was also recorded for each POAP film. As the electrode area and the thickness of the POAP films employed in SR were the same as those used in CV, RDEV and EIS measurements, the evolution of the voltammetric response with storage was practically the same as that shown in Fig. 1.

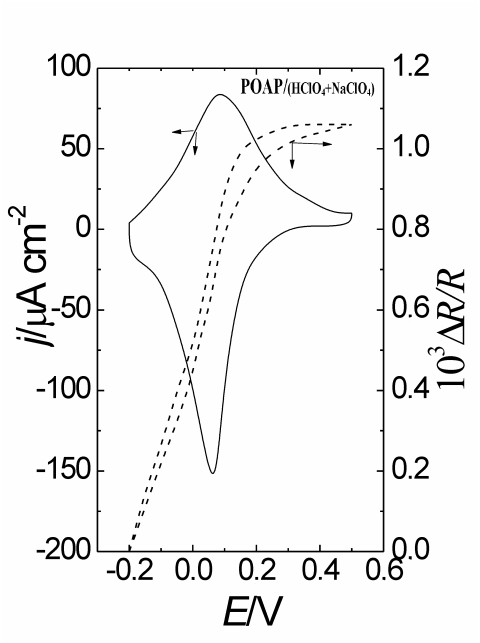

Fig. 28. Simultaneous $\Delta R/R$-E and j-E responses of a 30 nm thick gold film coated with a 2.8 mC cm^{-2} (ϕ_p = 60 nm) thick POAP film. Electrolyte: 0.1 M $HClO_4$ + 0.4 M $NaClO_4$. Scan rate: ν = 0.01 V s^{-1}.

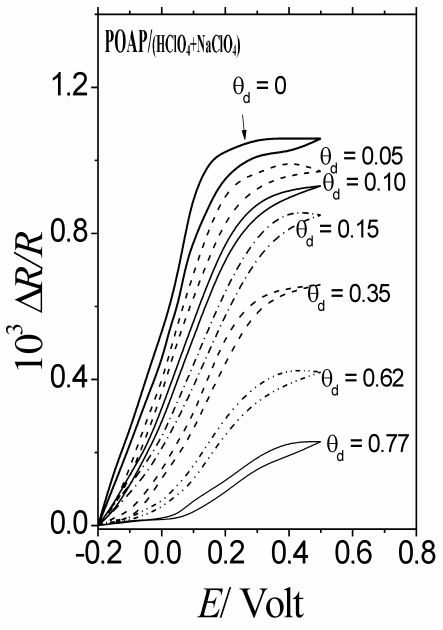

Fig. 29. *ΔR/R-E* responses obtained simultaneously with the (*j-E*) responses shown in Fig. 1. The degrees of deactivation are indicated in the figure (see also Table 1). Thickness of the gold film ϕ_m = 30 nm, resistance value of the gold film, R = 20.02 ohm. Thickness of the POAP film, ϕ_P = 60 nm. Electrolyte: 0.1 M $HClO_4$ + 0.4 M $NaClO_4$. Scan rate: ν = 0.01V s^{-1}.

With regard to *ΔR/R* vs. *E* response, the potential drop along the thin gold film electrode was compensated at the reduced state of POAP (*E* = -0.2 V) (see 'Materials and Methods' section). Then, an increase in the SR of the POAP-coated gold electrode is recorded as going from -0.2 V to 0.5 V. The increase in the gold film resistance during the transition from the reduced state to the oxidized state of a nondeactivated POAP film (Fig. 28) was explained in terms of the generation of electronic entities at the polymer chains near the electrode surface, which occurs by electron transfer across the polymer|metal interface [12]. In this connection, the redox switching of POAP was interpreted in terms of the oxidation of the amino groups to imine [6]. It is not unreasonable to expect that imine sites act themselves as different scattering centres compared with amine sites, increasing in this way the diffuse reflection of conduction electrons on the gold surface during POAP oxidation (increase of the resistance) [35]. That is, the *ΔR/R* increase in going from *E* = -0.2 V to *E* = 0.5 V in Fig. 28 can be explained in terms of a *p* decrease (Eq. (17)). With respect to the polymer redox conversion at the gold film surface, one has to keep in mind that the resistance changes at metal films are not the direct result of the electron transfer between the species on the metal film surface and the metal but they rather originate from the effect of foreign surface entities on the conduction electrons of the metal itself. On the other hand, as the potential drop along the resistive electrode (R ~ 20.02 ohm for ϕ_m = 30 nm) due to the measuring current I_m (see 'Materials and Methods' section) is compensated only *ΔR* changes associated to interfacial phenomena are recorded. Thus, the measured resistance change for a POAP-coated gold film electrode is only related to an interfacial (metal|polymer) electron dispersion process occurring during the reduction-oxidation process of the polymer film. The increase in *ΔR/R* during POAP oxidation can be explained in terms of an interfacial distribution of scatterers (imine sites) in the oxidised state with a spacing among them larger than that corresponding to amine sites in the reduced state [6, 12]. That is, the distribution of imine species in the oxidized state of POAP should be less compact than the corresponding distribution of amine species in the reduced state, which should lead to a more diffuse reflection of conduction electrons at the gold|POAP interface (lower specularity parameter at the oxidized state as compared with the value at the reduced one $p_{ox} < p_{red}$) [12]. A confirmation that supports a more extended configuration of oxidized sites, as compared with that of reduced ones, at POAP can be given in terms of gaps, which appear during POAP oxidation. In this respect, optical measurements on POAP films reveal that only one in every four or five amine sites is converted to the corresponding imine site [6]. Thus, the existence of inactive gaps within the distribution of oxidized sites of POAP could justify that POAP in its oxidized state reflects conduction electrons of gold more diffusely than in its reduced state. Further confirmation about the different reflecting properties of the oxidized and reduced states of POAP can be found in the different values of the site interaction parameters (*r*) obtained from the cathodic and anodic voltammetric response of POAP. A nonideal behaviour of POAP, which is actually expected

considering the rather high concentration of active sites in the film (*i.e.*, c = 4.7 M [1, 2]), leads to the following values of anodic and cathodic site interaction parameters: r_a = -0.55 M^{-1} and r_c = -0.18 M^{-1}, respectively. Both are negative, thus involving a repulsive energy of interaction. As a higher repulsion is observed between oxidized sites than between reduced ones at POAP, a more extended configuration of oxidized sites should be expected as compared with the corresponding distribution of reduced sites.

With regard to POAP deactivation after storage, as can be seen from Fig. 29, the more deactivated the POAP film becomes the more attenuated is the $\Delta R/R$ change in going from the reduced to the oxidized state of POAP. As indicated above, the measured resistance change is only related to an interfacial (metal|polymer) electron dispersion process which occurs during reduction-oxidation of the polymer film. This fact was proved by changing the POAP film thickness (Fig. 30). Fig. 30 shows that after increasing the POAP film thickness between 50 nm to 69 nm, the $\Delta R/R$ change remains practically the same. Obviously, the voltammetric responses (not shown) depend on the POAP thickness. However, the $\Delta R/R$ vs. E change, at constant POAP film thickness, depends on the gold film thickness (Fig. 31). That is, the thinner the gold film is (see Eq. (17)) the higher the ΔR value, and then, the resistance $\Delta R/R$ change becomes more pronounced (compare Figs 29 and 31 for the same θ_d values). Although the absolute resistance value, R increases as the metal film thickness decreases, the interfacial effects in the $\Delta R/R$ change become magnified as the thickness of the gold film decreases. In this regard, the lower the metal film thickness is, the more sensitive the SR technique becomes to study interfacial phenomena. This effect is quantitatively shown in Fig. 32, where the maximum $\Delta R/R$ change in going from -0.2 V to 0.5 V was represented as a function of the degree of deactivation of the POAP film for two different gold film thicknesses.

Although the absolute values of the specularity parameters at the reduced and oxidized state of POAP at each degree of deactivation are unknown (both parameters should depend on the degree of POAP deactivation), by employing Eq. (17), one can obtain the specularity parameter change (Δp) in going from the reduced to the oxidized state of POAP at each degree of deactivation. The Δp vs. θ_d dependences for the two different gold film thickness indicated in Fig. 32 are shown in Fig. 33. The following values were employed in Eq. (17)

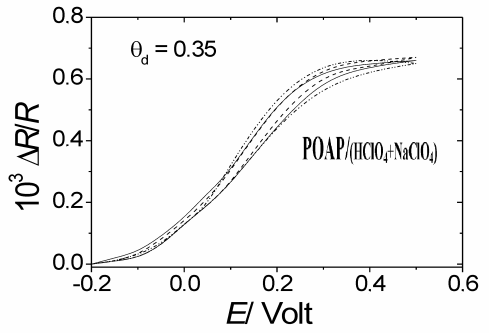

Fig. 30. $\Delta R/R$-E responses of a deactivated POAP film (θ_d = 0.35) deposited on a 30 nm thick gold film. Thicknesses of the POAP films: (- - -) ϕ_P = 69 nm; (—) ϕ_P = 60 nm; (— ·· —) ϕ_P = 52 nm. Electrolyte: 0.1 M $HClO_4$ + 0.4 M $NaClO_4$. Scan rate: ν = 0.01V s^{-1}.

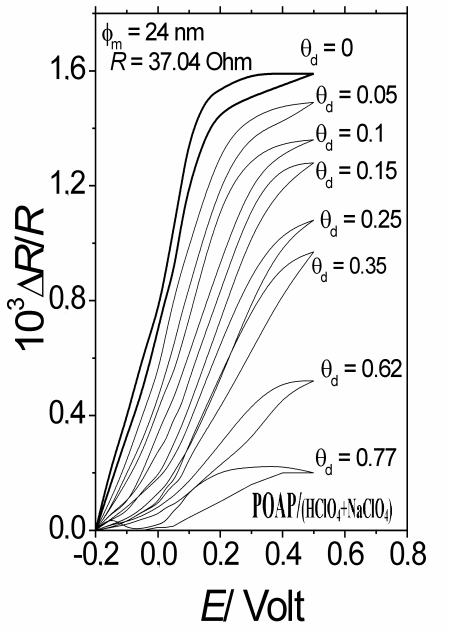

Fig. 31. $\Delta R/R$-E responses of a POAP-coated gold film electrode. Thickness of the POAP film, ϕ_P = 60 nm. Thickness of the gold film ϕ_m = 24 nm, resistance value of the gold film, R = 37.04 ohm. (θ_d = 0). A nondeactivated POAP film. Curves with θ_d values higher than 0 correspond to different deactivated POAP films indicated in Table 1. Electrolyte: 0.1 M $HClO_4$ + 0.4 M $NaClO_4$. Scan rate: ν = 0.01V s^{-1}.

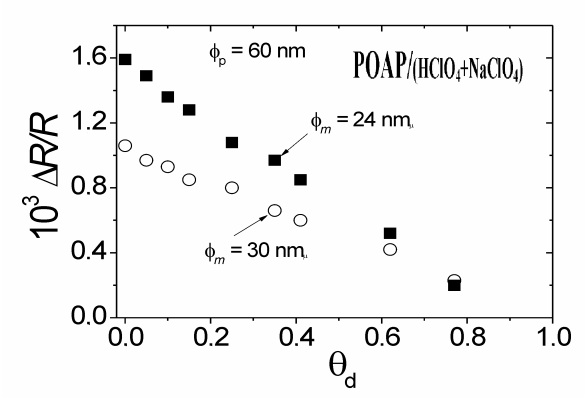

Fig. 32. Maximum $\Delta R/R$ change in going from the reduced to the oxidized state of POAP as a function of the degree of degradation, θ_d. Thickness of the POAP film, ϕ_P = 60 nm. Thickness of the gold film, ϕ_m: (O) 30 nm; (■) 24 nm.

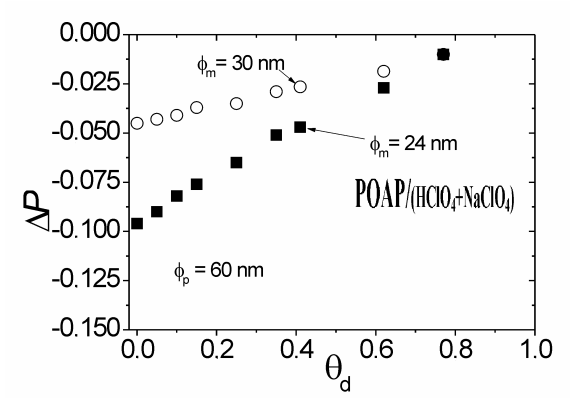

Fig. 33. The Δp vs θ_d dependence for the different gold film thicknesses: ϕ_m = 30 nm; ϕ_m = 24 nm. The corresponding resistances are: R = 20.02 ohm; R = 37.04 ohm.

to calculate Δp: l_m (= 22 nm at 25°C) is the mean free path of the conduction electrons of gold, ρ_m (= 2.4 x 10^{-6} ohm cm) is the bulk resistivity of the massive metal (gold) of the same structure as the metal film, ϕ_m is the thickness of the metal film, G (= 2) is the relationship between the length l and the width w of the rectangular gold film on which the POAP film was deposited. The resistance values R of the gold films are experimentally obtained. As indicated above, Δp is always negative, that is, $p_{ox} < p_{red}$. However, as can be seen from Fig. 33, as the degree of deactivation increases, Δp tends to increase. The maximal difference in the reflecting properties of the POAP|gold interface for the conduction electron of gold between the reduced and the oxidized states of POAP occurs for a nondeacitvated POAP film; however, the reflecting properties of the POAP|gold interface at the reduced and oxidized state of POAP tend to match as the degree of deactivation increases. This finding seems to be indicative of a redox site distribution that changes as the polymer becomes more deactivated. This change in the redox site distribution could explain the change in the electron hopping distance between redox sites, as is proposed in RDEV and EIS measurements to explain the changes of the charge-transport parameters (i.e. diffusion coefficients) with the degree of deactivation. As can be seen from Fig. 33, the lower the thickness of the gold film is, the more pronounced the Δp change at the gold|POAP interface becomes at each degree of deactivation. As indicated above, this effect is due to the higher sensitivity of the SR technique to detect surface phenomena as the metal film thickness decreases.

At this point a comparison between $R_{m|f}$ and $\Delta R/R$ changes with the degree of deactivation (Figs. 13 and 32, respectively) can be established. While the increase in $R_{m|f}$ during the deactivation of the polymer film could be associated with a transversal resistance due to the electron transfer across the polymer|metal interface, the $\Delta R/R$ decrease with POAP deactivation can be attributed to the scattering of conduction electrons at distributions of redox sites of different compactness (different distances between active sites). Despite both resistances are associated to the redox site distribution at the metal|POAP interface, it should be taken into account that while the $\Delta R/R$ change (-0.2 V to 0.5 V) is obtained from a potentiodynamic technique (CV), $R_{m|f}$ is extracted at the reduced state of POAP employing EIE. Then, while the increase in $R_{m|f}$ is associated to an increase in the amount of inactive redox sites at the reduced state during POAP deactivation, the $\Delta R/R$ decrease could be attributed to the change in the reflecting properties of the redox site distributions at the reduced and oxidized states of POAP for the conduction electrons of the gold film which tend to match as the polymer becomes more deactivated.

CONCLUSIONS

Different electrochemical and chemical treatments at which poly(*o*-aminophenol) films are subjected in both basic and applied research affect their conducting properties. In this work it is demonstrated that poly(*o*-aminophenol) films maintain their conducting properties unaltered even after a storage time without use of one day. However, a loss in conductivity was observed as the storage time was extended beyond 30 h. This loss of conductivity was studied by CV, RDEV, EIS and SR measurements. An attenuation of the voltammetric response of POAP is observed with the increase in the storage time. This attenuation allows one to define a degree of deactivation of the polymer. Dependences of conduction parameters on the degree of deactivation were obtained in the presence of an electroactive solution employing RDEV and *ac* impedance measurements. The electron hopping model was employed to interpret RDEV experiments. EIS data were interpreted on the basis of a model which allows one to explain both ionic and electronic interfacial exchange across the POAP|solution interface. EIS data obtained in the presence of only the supporting electrolyte were interpreted employing a modified electron-hopping model, which considers a protonation reaction coupled with a self-exchange process between oxidized and reduced sites. Parameters extracted from both models were compared. While electron (D_e) and ion (D_i) diffusion coefficients decrease, interfacial resistances ($R_{m|f}$, $R_i^{f|s}$, $R_e^{f|s}$) increase as the degree of deactivation of the polymer increases. The slower electron transport with the increase in the degree of deactivation was attributed to the increase in the electron hopping distance between redox sites. While parameters representing electron motion extracted from RDEV and impedance measurements seem to change continuously within the whole range of deactivation degree, parameters representing the ion transport show a break at a degree of deactivation of about 0.35. This characteristic of the ion transport at POAP was associated with the existence of two forms of hydrogen ions in the POAP film.

The relative surface resistance change of a thin gold film coated with poly(*o*-aminophenol) is gradually attenuated with the increase in the storage time. The surface resistance change in going from the reduced to the oxidized state of POAP was attributed to a change from specular to diffuse scattering of conduction electrons from the inside of the gold film to the POAP|gold film interface. The attenuation of the surface resistance change as the degree of deactivation of POAP increases was attributed to a change in the redox site configuration, which seems to be in agreement with the increase in the electron hopping distance between redox sites, proposed to explain the decrease in diffusion coefficient values obtained from RDEV and EIS measurements with the increase in the degree of deactivation.

The dependence of charge-transport and charge-transfer parameters on the degree of deactivation for POAP films deactivated employing different procedures, STWU, PPC, SFeIS and HPPL were compared in this work. While the deactivation of poly(*o*-aminophenol) films by soaking in a ferric ion solution has been attributed to the direct interaction of iron ions with the redox sites of POAP, which impedes the protonation reaction of the polymer, the loss of electroactivity of a polymer film under continuous potential cycling has been associated with the excessive uptake of redox sites by doping anions from the external electrolyte solution. Also, the effect of high positive potential limits on electroactive polymer conductivities has been associated with lateral reactions that could increase the residual saturation in polymeric chains, causing a strong reduction in the electron conduction through conjugated domains in large polymeric chains.

ACKNOWLEDGEMENTS

The author gratefully acknowledges the Consejo Nacional de Investigaciones Científicas y Técnicas (CONICET) and also the Facultad de Ciencias Exactas, National University of La Plata (UNLP).

CONFLICT OF INTEREST STATEMENT

The author declares no conflict of interest.

REFERENCES

1. Barbero, C., Silber, J. J. and Sereno, L. 1990, J. Electroanal. Chem., 291, 81.
2. Barbero, C., Silber, J. J. and Sereno, L. 1989, J. Electroanal. Chem., 263, 333.

3. Ohsaka, T., Kunimura, S. and Oyama, N. 1988, Electrochim. Acta, 33, 639.
4. Tucceri, R., Arnal, P. M. and Scian, A. N. 2013, Canadian Journal of Chemistry, 91, 91.
5. Scolari, D. and Tucceri, R., 2011, Micro and Nanosystems, 3, 115.
6. Tucceri, R. I., Barbero, C., Silber, J. J., Sereno, L. and Posadas, D. 1997, Electrochim. Acta, 42, 919.
7. Levin, O., Kondratiev, V. and Malev, V. 2005, Electrochim. Acta, 50, 1573.
8. Miras, M. C., Badano, A., Bruno, M. M. and Barbero, C. 2003, Portugaliae Electrochimica Acta, 21, 235.
9. Yano, J., Kawakami, H., Yamasaki, S. and Kanno, Y. 2001, J. Electrochem. Soc., 148, E61-E65.
10. Lobo, M. J., Miranda, A. J., López-Fonseca, J. M. and Tuñón, P. 1996, Analytica Chimica Acta, 325, 33.
11. Zhang, A. Q., Cui, C. Q. and Lee, J. Y. 1996, Electroanal. Chem., 413, 143.
12. Tucceri, R. 2004, Surface Science Reports, 56, 85.
13. Tucceri, R. I. 2001, J. Electroanal. Chem., 505, 72.
14. Tucceri, R. 2014, J. Electroanal. Chem., 717-718, 131.
15. Tucceri, R. 2005, Journal of new materials for electrochemical systems, 8, 305.
16. Tucceri, R. 2009, J. Electroanal. Chem., 633, 198.
17. Tucceri, R. 2011, J. Electroanal. Chem., 659, 83.
18. Vorotyntsev, M. A., Deslouis, C., Musiani, M. M., Tribollet, B. and Aoki, K. 1999, Electrochim. Acta, 44, 2105.
19. Barbero, C., Zerbino, J., Sereno, L. and Posadas, D. 1987, Electrochim. Acta, 32, 693.
20. Tucceri, R. I. and Posadas, D. 1983, J. Electrochem. Soc., 130, 104.
21. Andrieux, C. P. and Savéant, J. M. 1980, J. Electroanal. Chem., 111, 377.
22. Laviron, E. 1980, J. Electroanal. Chem., 112, 1.
23. Bonfranceschi, A., Pérez Córdoba, A., Keunchkarian, S., Zapata, S. and Tucceri, R. 1999, J. Electroanal. Chem., 477, 1.
24. Barbero, C., Tucceri, R. I., Posadas, D., Silber, J. J. and Sereno, L. 1995, Electrochim. Acta, 40, 1037.
25. Chidsey, Ch. E. D. and Murray, R. W. 1986, J. Phys. Chem., 90, 1479.
26. Vorotyntsev, M. A. 2002, Electrochim. Acta, 47, 2071.
27. Agarwal, P., Orazem, M. E. and García-Rubio, L. H. 1995, J. Electrochem. Soc., 142, 4159.
28. Orazem, M. E. 2004, J. Electroanal. Chem., 572, 317.
29. Musiani, M. M. 1990, Electrochim. Acta, 35, 1665.
30. Salavagione, H. J., Arias-Padilla, J., Pérez, J. M., Vázquez, J. L., Morallón, E., Miras, M. C. and Barbero, C. 2005, J. Electroanal Chem., 576, 139.
31. Bisquert, J. 2002, Electrochim. Acta, 47, 2435.
32. Rodríguez Nieto, F. J. and Tucceri, R. I. 1996, J. Electroanal. Chem., 416, 1.
33. Fuchs, F. 1938, Proc. Camb., Phyl. Soc. Math. Phys. Sci., 34, 100.
34. Sondheimer, E. H. 1952, Adv. Phys, 1, 1.
35. Tucceri, R. I. 2003, J. Electroanal. Chem., 543, 61.